Figure 24   Mineralization model of Bou Khil mine (N. Hatira, et. al., 1990)
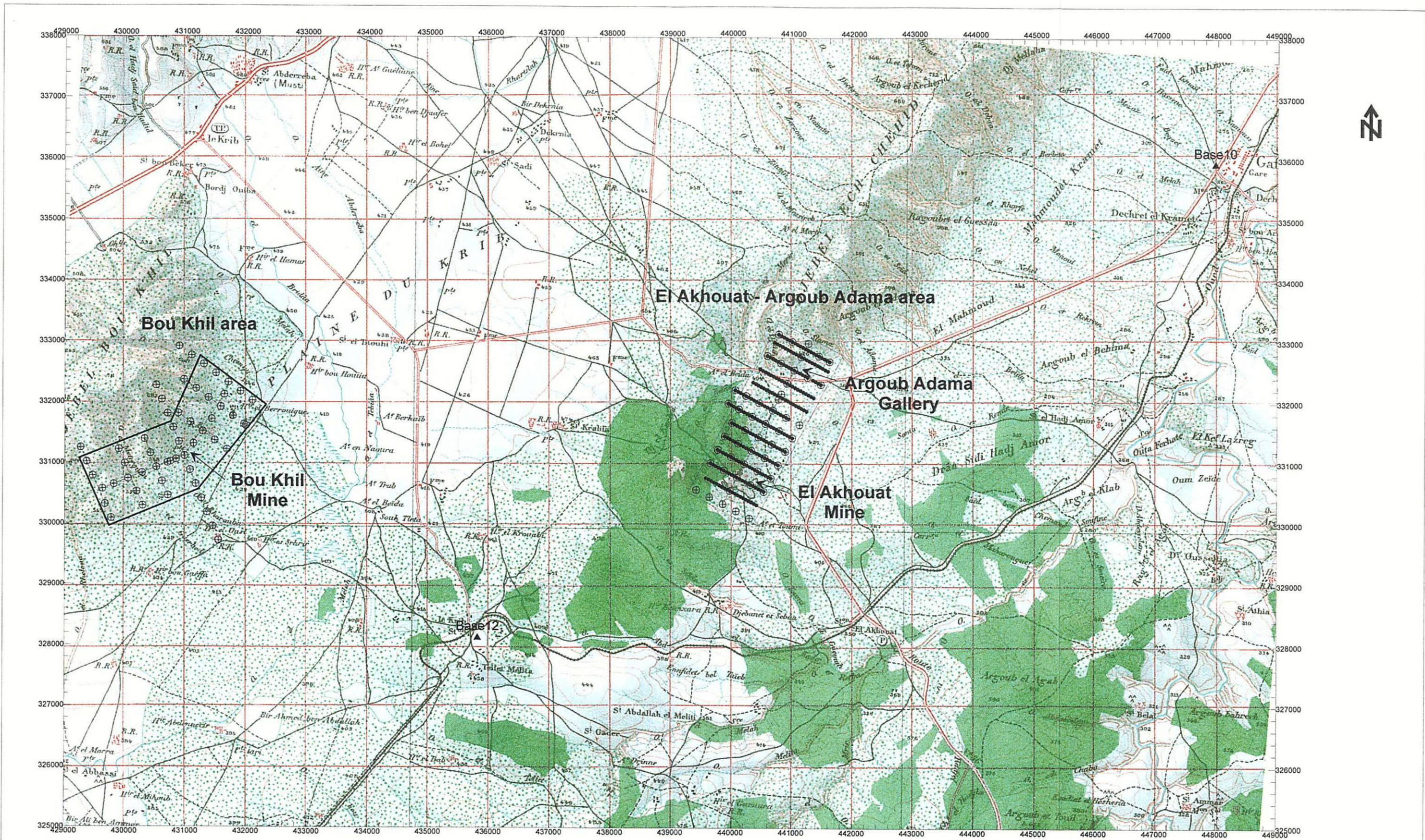
3.3   Geophysical Prospecting

In the Bou Khil prospect, geophysical surveys using a gravity and IP methods are carried out along 8 measuring lines with a total line length of 11.3 km covering an area of 3 km^2 as shown in Figure 25. The methodology and the results of the geophysical surveys are described below.

3.3.1 Methodology

(1) Layout of Measuring Lines

The 8 measuring lines, the line numbers from B0 through B7, are laid out by open traverse surveying using an electro-optical distance meter and a transit compass. Measuring stations are set along each line principally at an interval of 50 m and marked by wooden pickets. Each measuring station identifies itself by the number of relevant line and one tenth of the distance from the initial station of the line, that is, the measuring station B0-125 indicates its position at 1250 m from the initial station of the line B0. The specifications and locations of each measuring line are shown in Table 23 and Figure 26 respectively.

Bou Khil area

Bou Khil Mine

El Akhouat - Argoub Adama area

Argoub Adama Gallery

El Akhouat Mine

Base 10

Base 12

PLAINE DU KRIB

JEBEL BOU KHIL

JEBEL ECH CHEHID

Legend

▲ : Gravimetric Survey Base Station

⊕ : Gravimetric Survey Station

— : IP survey Line

• : Magnetic Survey Station

☐ : Survey Area

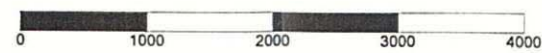0   1000   2000   3000   4000

Figure 25

Geophysical Survey Area Map

1 : 60,000

March, 2000

Legend

⊕ : Gravimetric Survey Station

—— : IP survey Line

▭ : Survey Area

╳ : Closed Mine

Figure 26

Layout of Geophysical Survey Line in Bou Khil area

1 : 25,000

March, 2000

Table 23 Specification of geophysical survey lines in Bou Khil area

Line	Stations	Length (km)	Angle	Crossing to B0	x(UTM)	y (UTM)	Applied Survey
B0	61 (0~300)	3	N70°E (0~150)		510421.53	4013933.07	Gravity IP
			N44°E (150~300)		512513.49	4015718.73	
B1	25 (0~125)	1.25	N20°W	B0-0	510612.25	4013470.89	Gravity IP
					510135.44	4014626.34	
B2	21 (0~100)	1	N20°W	B0-50	51120.61	4013680.68	Gravity IP
					510739.17	4014605.04	
B3	21 (0~100)	1	N20°W	B0-100	511536.60	4013852.33	Gravity IP
					511155.15	4014776.68	
B4	28 (-100-175)	2.75	N20°W	B0-150	512380.22	4013118.71	Gravity IP
					511331.26	4015660.67	
B5	21 (0~100)	1	N54°W	B0-200	512506.23	4014617.14	Gravity IP
					511696.15	4015203.39	
B6	23 (0~130)	1.3	N54°W	B0-250	512799.36	4015022.17	Gravity IP
					511746.25	4015784.30	
B7	5 (0~150)	1.5	N54°W	B0-300	510421.53	4015425.60	Gravity
					511703.41	4016304.98	

The baseline B0 with a total length of 3,000 m is set centering the old mine site of Bou Khil along the boundary between the Triassic and Cretaceous systems where ore bodies are located. Since the boundary is curving, the baseline, being bent at its middle, runs in the N 46° E direction from the initial station B0-0 at its southwestern end through the station B0-150 and then turns its direction in N 70° E between the stations of B0-150 and B0-300.

Other 7 measuring lines, principally 1,000 m long each, are laid out perpendicularly to the baseline at an interval of 500 m with the initial stations at their southeastern ends. The 3 lines, B1 at the southwestern end and B6 and B 7 in the northeastern most of the baseline, are extended for distances of 250-500 m northwestwards. The line B4, which crosscuts the baseline at its middle in the vicinity of the old mine site of Bou Khil, is also extended for a distance of 750 m northwestwards.

The coordinates of these measuring lines are correlated by surveying to the base station which has been located in the vicinity of the old mine site of Bou Khil by ONM. Since the coordinate system used for the surveying is the northern Tunisia surveying coordination by the Lambert Projection (hereinafter called Lambert Coordinate System), all coordinates are transformed to the UTM (Universal Transverse Mercator Projection) and the Geographical Coordinate Systems with the courtesy of ONM. Of all outputs of the current investigation, the geophysical maps are prepared in accordance with the Lambert Coordinate System, on which all existing topographic, geologic, regional Bouguer anomaly maps are based. The elevation of each measuring station is determined by leveling using a digital auto-level, Model SDL30-1,

manufactured by Sokia Co., Ltd., in order to achieve the accuracy of 10 cm $\pm$ required for the gravity survey. The leveling is carried out based on the elevation base station, located near the old mine site of Bou Khil by ONM.

(2) Gravity Survey

The gravity measurement is taken principally at an interval of 250 m along all 8 measuring lines laid out in the Bou Khil prospect as above explained. In the neighboring area, the gravity survey project, CG-02, was carried out with a density of one measuring point for an approximately one square kilometer by ONM in 1998. Its result is published in gravity Bouguer anomaly maps at a scale of 1 to 50,000, which are also compiled to an 1 to 200,000 scale map. The Bou Khil prospect of the current program is located at the western end of the Gafour gravity quadrangle.

Relative gravity to that at the known station is measured using a gravimeter, Model D with a detection accuracy of 0.1 μ gal, manufactured by La Coste & Romberg Co., Ltd. Prior to the commencement of gravity survey, the gravimeter is verified for the coefficient of conversion of its readings to gravity values by taking measurements twice at the gravity base stations 9, 10 and 12 for the Project CG-02. The result of verification, presented in Table 24, proves that the coefficient used traditionally is valid for the conversion in the current survey. The station 12 of the project CG-02 is selected for the gravity base station of the current survey because of its convenient location and ground stability for steady gravity measurements. Gravity is measured once or more every day at the gravity base station for each closing gravity traverse. The maximum error for one closing gravity traverse is recorded at 0.1 mgal throughout the current survey.

Table 24   Results of Rock Density measurement of specimens in Bou Khil area

Base	UTM Coordinate		Gravity Value (mgal)			Error (mgal)
	x	y	observed	averaged	known	
9	537807.754	4008955.329	979730.81 / 979730.84	979730.83	979730.69	0.14
10	528783.844	4019481.981	979774.53 / 979774.53	979774.53	979774.53	0.00
12	516702.659	4004998.969			979741.99	

A gravity value, ABSG (mgal), at each measuring station is estimated using a relative gravity, RG, at the measuring point and the gravity value, ABSG, at the gravity base station as follows:

ABSG(measuring point) = RG(measuring station) − RG(base) + ABSG(base)   (1)

where

RG = reading x factor + C_{inst} + C_{tidal} + C_{drift} (2)

reading: instrumental reading, factor: reading — coefficient of conversion

C_{inst}: correction for instrument height, C_{tidal}: tidal correction

C_{drift}: drift correction.

A Bouguer gravity value, Ab (mgal), is also estimated for each measured gravity value (ABSG) using the following equation;

$$Ab = ABSG - G_{stand}(\phi) + C_{atm}(h) + C_{free}(h) + Cb(h, \gamma) + T(h, \gamma) \tag{3}$$

ϕ : latitude of measuring point, h: elevation of measuring point(m)

γ : specific gravity of rocks in the vicinity of measuring point(g/cm^3)

where

● Standard Gravity Value (1967 formula)

$$G_{stand}(\phi) = 978031.85(1 + 0.005278895 \sin^2 \phi + 0.000023462 \sin^4 \phi) \tag{4}$$

● Atmospheric Correction

$$C_{atm}(h) = 0.87 - 0.000965 \, h \tag{5}$$

● Free-air Correction

$$C_{free}(h) = (\delta g / \delta h) \times h = 0.3086 \, h \tag{6}$$

● Bouguer Correction

$$Cb(h, \gamma) = -2\pi G \gamma h = -0.04192 \gamma h \tag{7}$$

π : circular constant, G: universal gravitation constant

● Topographic Correction: $T(h, \gamma)$

adopting the Topographic Correction Formula of GSJ (Geological Survey of Japan), established in 1989 by its Gravity Survey Research Group.

The density in the vicinity of measuring stations, which is used for the Bouguer and topographic corrections, is usually determined by an appropriate judgement taking account of densities estimated according to the following means;

① the result of density measurement of rock samples.

② the gradient of G-H correlation diagram.

G-H correlation diagram (Figure 27): produced by plotting measurements on a diagram with the abscissa for the differences between measured and standard gravity values against the ordinate for the elevation differences between measuring points.

③ comparison of the topographic map with Bouguer anomaly maps for several assumed densities: selecting the density least correlated to the topography.

A density of 2.29 g/cm^3 is obtained on the basis of the G-H diagrams for the Bou Khil and El Akhouat prospects. Besides, the Bouguer anomaly maps for the densities of 2.3 and 2.4 are judged to be relatively low in their correlativity with the topographic map. Taking these results into consideration, the correction density of 2.33 g/cm^3, used in the Project CG-02, is adopted in the current gravity survey for the
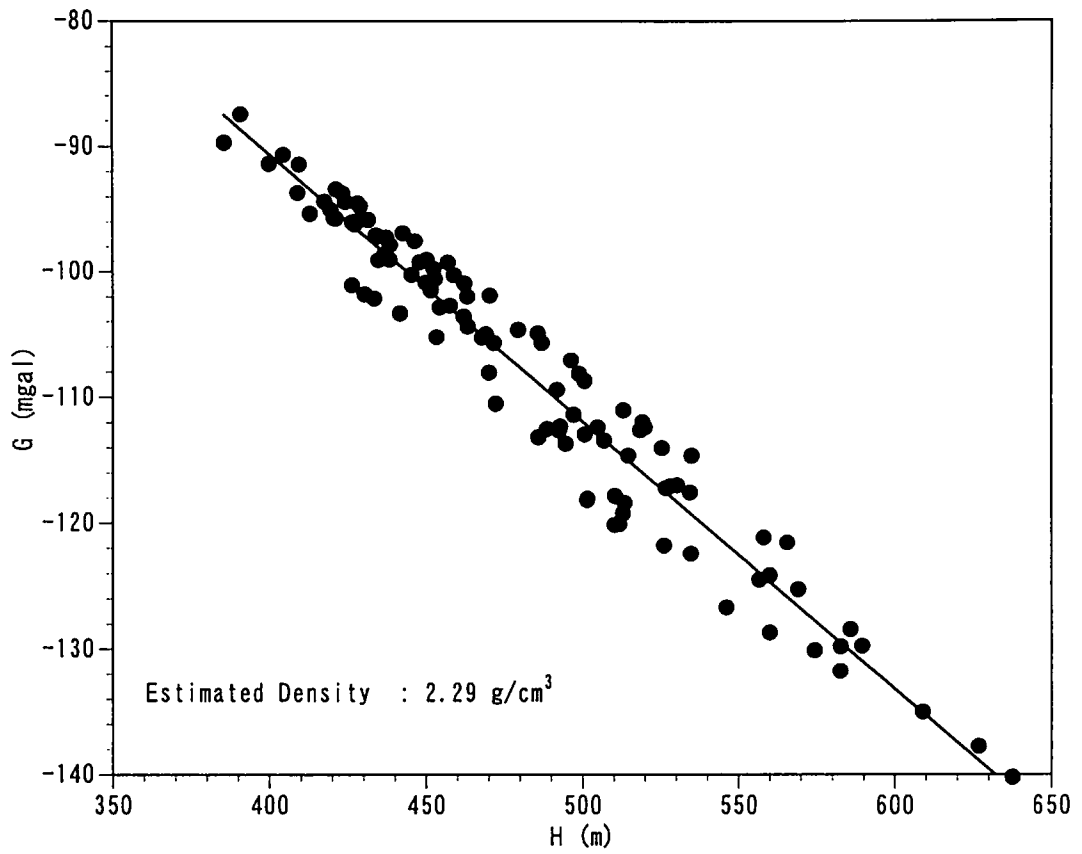
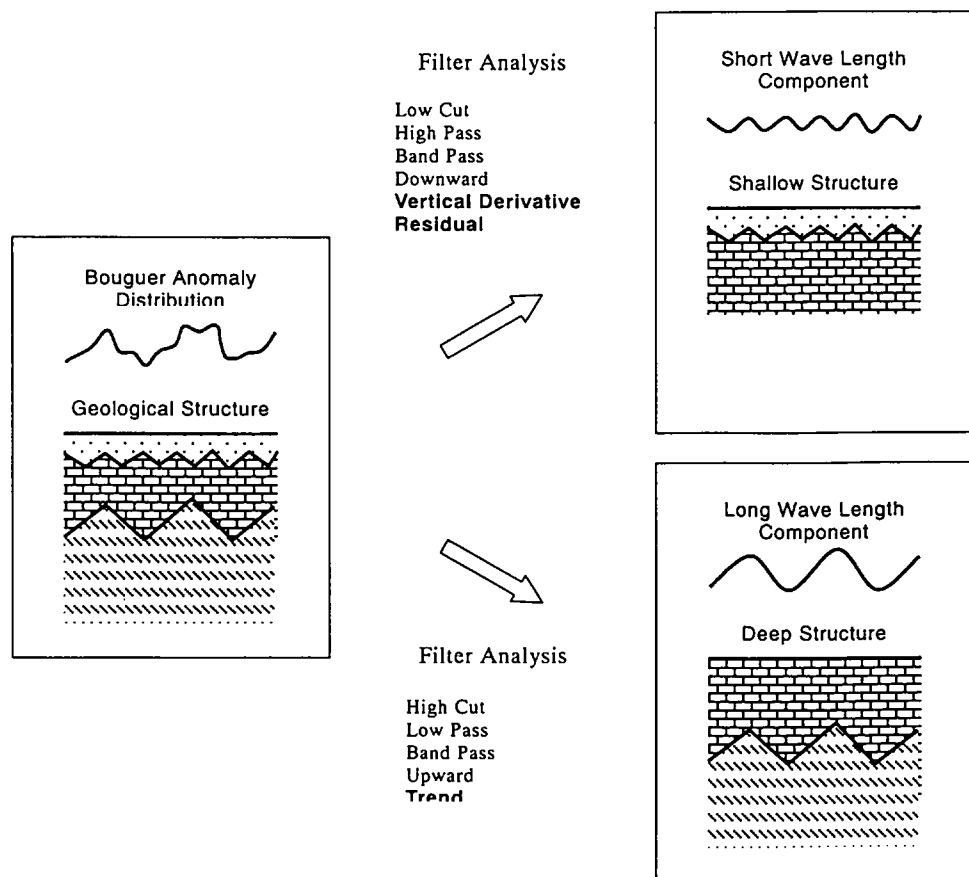Figure 27 G-H Correlation Diagram

Figure 28   Schematic Diagram of Filter Analysis
in Gravimetric and Magnetic Surveys

purpose of comparison. The Bouguer anomaly map (gravity contour map), indicating a horizontal distribution of Bouguer gravity values, is shown in Figure 40.

Horizontal distribution of Bouguer gravity values comprises composite of shorter and longer spatial wavelength variations of gravity in the region as illustrated in Figure 28. The shorter wavelength variation reflects density variation of rocks in the shallower part of earth and the longer wavelength variation, that in the deeper part, several kilometers or deeper from the surface. The Bouguer gravity values of the Bou Khil prospect, after estimation of 2-dimensional Fourier transform, are plotted on the power spectrum diagram (Figure 29) with the abscissa for wave number (spatial frequency) against the ordinate for natural logarithm of spectrum power. According to the diagram, the Bouguer gravity anomaly of the prospect is composed of three components with their average depths at 927 m, 188 m and 51 m. Since the current gravity survey is concerned with prospecting ore deposits shallower than a few kilometers, it is tried to extract a shorter wavelength, that is, shallow component from the Bouguer anomaly map.

For extracting the shorter wavelength component, one approach is to use a low-cut or band-pass filter for data processing and the other, to estimate residuals over a regional trend surface of Bouguer gravity values. In the current survey, the first vertical derivative filter, a kind of low-cut filter, and the trend surface analysis are adopted for extracting the shorter wavelength component.

The result of first vertical derivative filtering is shown in the first vertical derivative anomaly map (Figure 39). The 0 contour between the positive maximum and the negative minimum indicates a boundary between two subsurface geologic bodies with different density structures, e.g. a fault, a intrusive contact, etc., as shown in Figure 30.

In general, a trend surface is mathematically approximated by an n-dimensional polynomial or is obtained using a low-pass filter such as the upward continued filter. Where measuring stations are sparsely located, the shorter wavelength component tends to be also filtered out. Therefore, the Bouguer anomaly distribution of the CG-02 Project (Figure 39), in which the number of measuring stations per unit area is one quarter of the current survey or less, is utilized as the trend surface for estimation of residuals. The result of residual estimation is illustrated in the residual gravity anomaly map (Figure 41).

A profile analysis along the 7 measuring lines, B0 through B6, is made so that the gravity residuals match with the subsurface density structures along these measuring lines. The model profiles of subsurface density structures, as the result of profile analysis, are shown in Figure 43 through 48. The best-fit models for given
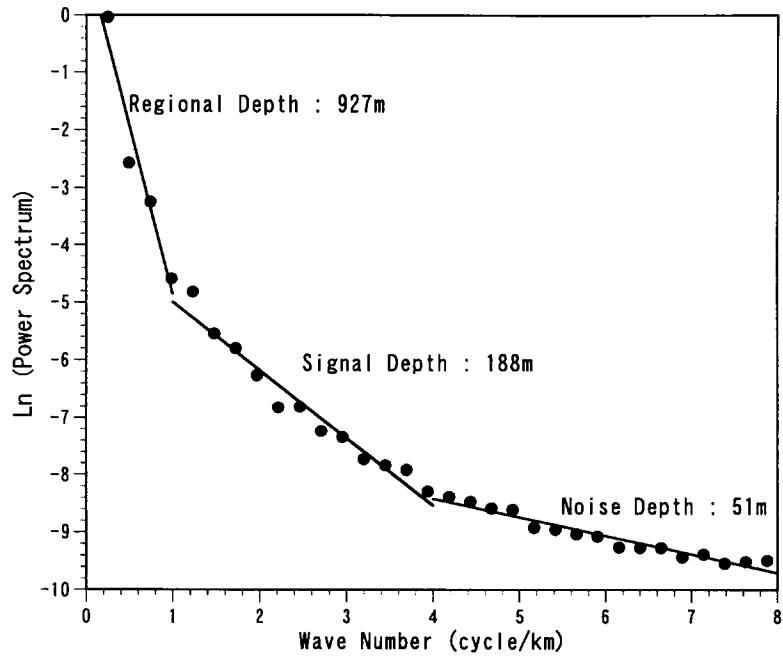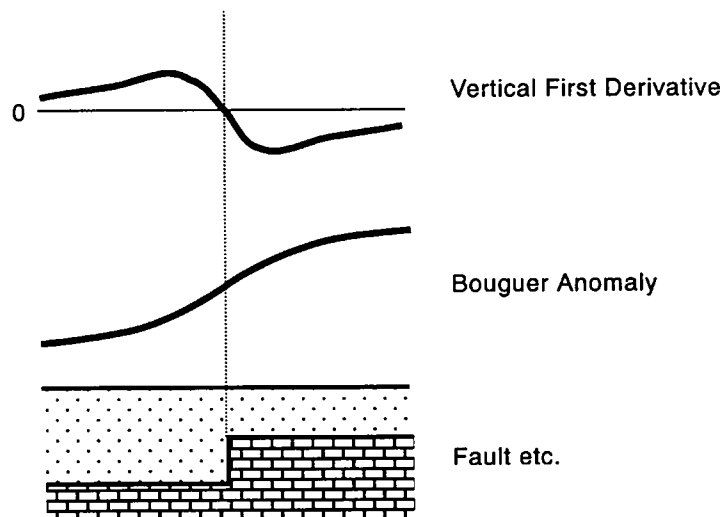
Figure 29 Power Spectrum diagram in Bou Khil area

Figure 30 Enhancement of Vertical First Derivative

residuals are interactively approximated for its size and density structure, using the software for magnetic and gravity profile analysis, GM-SYS (Version3.6), developed by Northwest Geophysical Associates Co., Ltd. in USA. Then, the approximated best-fit models are further refined inversely by computing its size and density structure directly from the residuals. The standard gravity residuals are read on the residual gravity anomaly map. The densities for the subsurface models are expressed in their differences against the correction density, 2.33 g/cm³.

(3) IP Survey

The IP survey is carried out for the 7 measuring lines, B0 through B6, according to the following specifications. The line B0 is surveyed for the entire 3 km, while the measurement is made only for the northwestern end 1 km, toward the hill, of each of the other 6 lines.

- Electrode Configureuration: Dipole-Dipole Array
- Electrode Spacing (a): 100 m
- Electrode Separation Index (n): 1 to 5
- Transmitted Current: Frequency = 0.125 Hz, Square-Wave with 50 % Duty Cycle
- IP Method: Time Domain
- Equipment   Generator: Honda, Model ET4500

    (Max. Output = 4.5 kVA, 3-Phase Alternate, 200 V)

    Transmitter: Chiba Electronic, Model CH-400

    (Max. Output = 1000 V − 10 kVA)

    Transmission Controller: Zonge Engineering (USA), Model XMT-32

    Receiver: Zonge Engineering (USA), Model GDP-32 (Accuracy = 1μ V)

The transmitting dipole, C1-C2, is stationed in the southeastern plain side of the survey area, while each of the 5 receiving dipoles, P1-P2, P2-P3, P3-P4, P4-P5 and P5-P6 is disposed at a pair of measuring stations in the northwestern hill side. The measurement is made spontaneously at these receiving dipoles. Variation in voltage received at each dipole is shown in Figure 31. Apparent resistivity ρ a(Ω m) is estimated, according to the equation (8), for the primary voltage V_p(V) that is the voltage stabilized at a certain level after current I(A) is transmitted.

$$\rho a= KV_p/I \tag{8}$$

where K is electrode configuration factor which is estimated for the dipole-dipole array used in the current survey according to the equation (9).

$$K= n(n—1)(n—2) \pi a \tag{9}$$

a: electrode spacing(m), n: electrode separation index

Chargeability M (mV/V or o/oo) is estimated, according to the equation 3.3-9,

for the secondary voltage Vs(t)(unit: mV) that is a decayed voltage measured at a certain elapsed time after current shut-off. The integration range (t1=450msec to t2=1100msec) for chargeability estimation corresponds to that of the Newmont standard which is normally used in the time domain IP method.

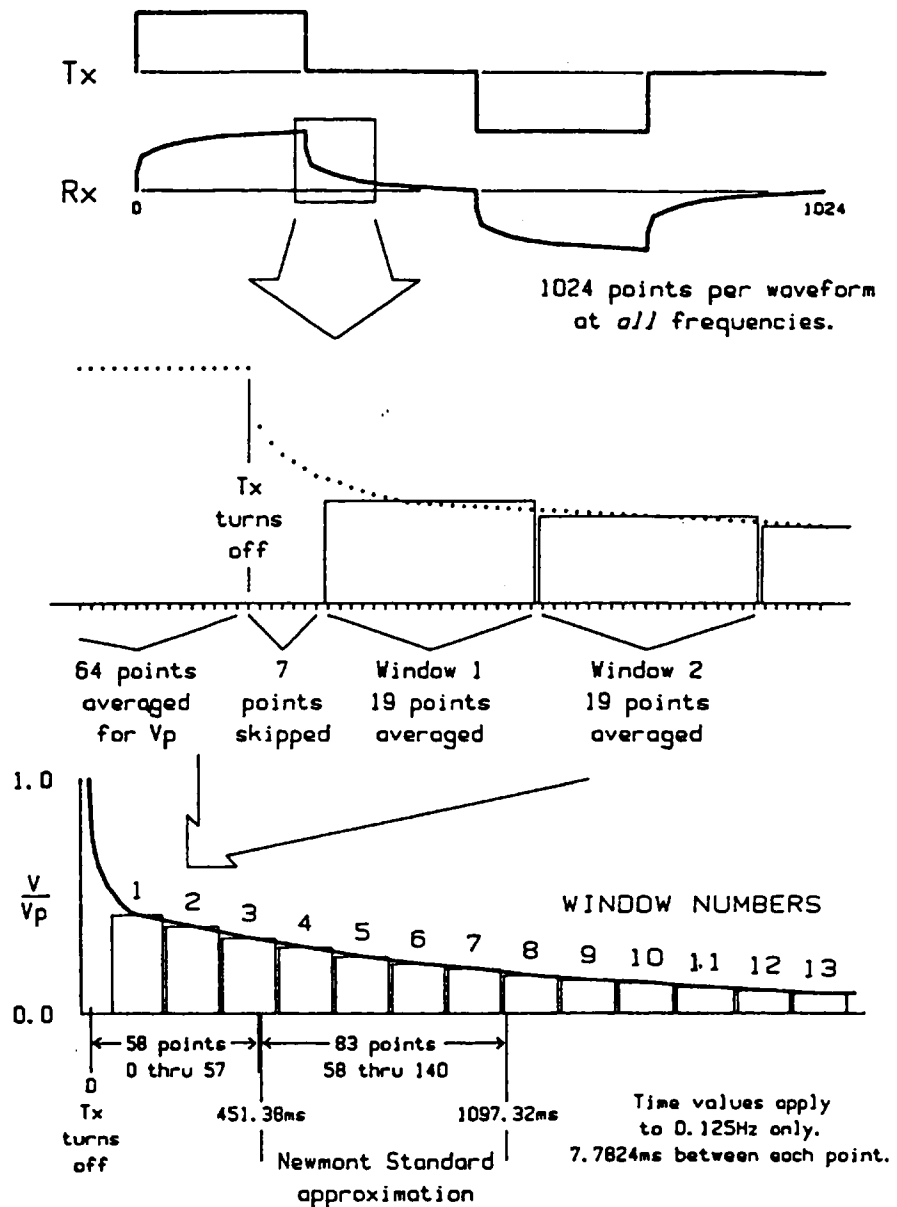$$M = \frac{1}{Vp\,(t1-t2)}\int_{t1}^{t2} Vs(t)\,dt \tag{10}$$

Figure 31　Schematic diagram of time domain IP with GDP-32
(Zonge Engineering, 1994)

In case of Model GDP-32 of Zonge Engineering, one wave-form comprises 1,024 data points. Therefore, the data for the adopted frequency of 0.125 Hz are acquired at an interval of approximately 7.7824 msec (millisecond). While the primary voltage V_p is practically given as a mean of 64 data before current turn-off, the voltage decay curve consists of 13 voltage windows, each of which is given as a mean of 19 point data. GDP-32 computes, at the time of measurement, the chargeability of Newmont standard, Ms (unit: msec), using the equation 11. The chargeability of Newmont standard is then converted to the IP measurement, M, using the equation 12.

$$Ms = (T/1024) \times 1.87 \times 19 \times (W4+W5+W6+W7+W8+W9) \qquad (11)$$

Where, T : period of transmitting current (msec)

Wn : Normalized decay voltage in n-number window (mV/V)

$$M = Ms *1024/(T \times 1.87 \times 19 \times 4) \qquad (12)$$

Eight wave-forms are collected at one measurement and compared to each other, in order to upgrade S/N (signal/noise) ratio. Although considerable current, ranging from 0.3 to 10 A, is applied, observed V_p seldom exceeds 1mV due to extremely low ground resistivity. Where V_p is low as is the case, reproducible data can be obtained for apparent resistivity. However, it is very difficult to obtain smooth voltage decay curves as shown in Figure 32. Measurements are repeated three to four times at one measuring station in order to obtain voltage decay curves with acceptable smoothness.
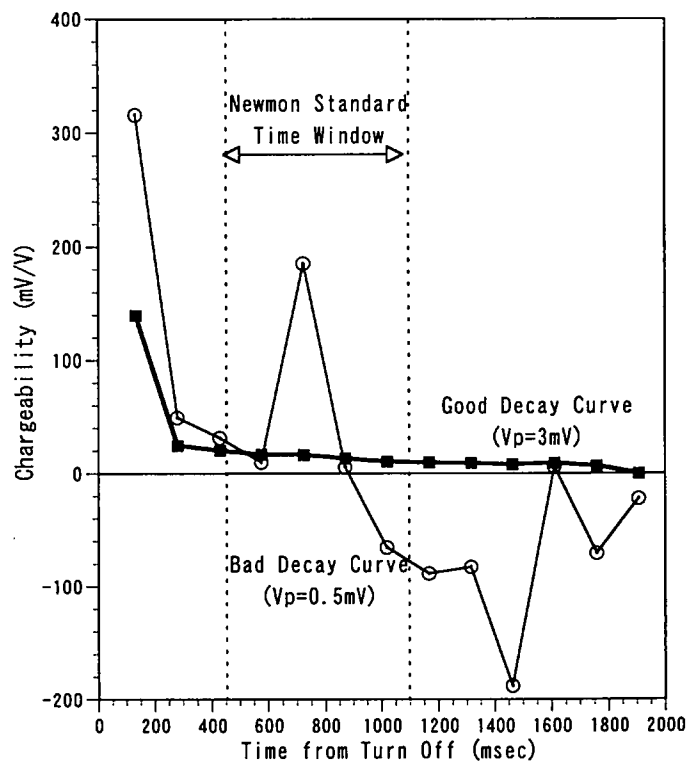
Figure 32   Example Observed Decay Curves

The measured apparent resistivity and chargeability, as well as the voltage decay curves, are presented in Figure 33. Pseudo-cross sections of apparent resistivity and chargeability for each measuring line are shown in Figures 50 through 56. Based on these pseudo-cross sections, apparent resistivity and chargeability contour maps for the electrode separation indices, n =1,2,3 and 4, are prepared according to the plotting procedure illustrated in Figure 33. These plans for apparent resistivity and chargeability are shown in Figures 57 through 60 and Figures 61 through 64. An anomaly on a pseudo-cross section does not indicate actual geometry of a causative body as shown in Figure 33. It is, therefore, necessary to interpret the anomaly by 2-dimensional modeling analysis for geometry of a causative body on the relevant cross section. In the current investigation, field data are interpreted by combination of the 2.5 dimensional FEM (Finite Element Method) modeling and inversion using the constrained non-linear regression method as proposed by Sasaki (1992). The 2.5 dimensional FEM modeling proposed by Coggon (1977) assumes a prismatic model perpendicular to a cross section extending for a infinitive distance and estimates 3-dimensional voltage distribution applying the Fourier transformation over the assumed prismatic model in accordance with actually transmitted current. This modeling method, combined with inversion, has been put into practical use by Pelton, et al. (1978). Since inversion of apparent resistivity often becomes ill-conditioned, the constraint, called 'Laplacean', is stipulated for its application in order to obtain stable solutions (Dey, et al., 1979). Therefore, the result of inversion is reliable for distribution of apparent resistivity, however, may not necessarily provide absolute values of apparent resistivity or chargeability. Figure 35 indicates elements of FEM used in the cross section analysis and an example of a block interpreted by inversion. A flow of inversion is shown in Figure 36. Interpreted apparent resistivity and chargeability are plotted on cross sections of measuring lines and are illustrated with contours in Figures 65 through 71. Contour plans of interpreted apparent resistivity and chargeability for elevations at 200, 300 and 400 m above mean sea level are shown in Figures 72 through 74 and Figures 75 through 77 respectively.
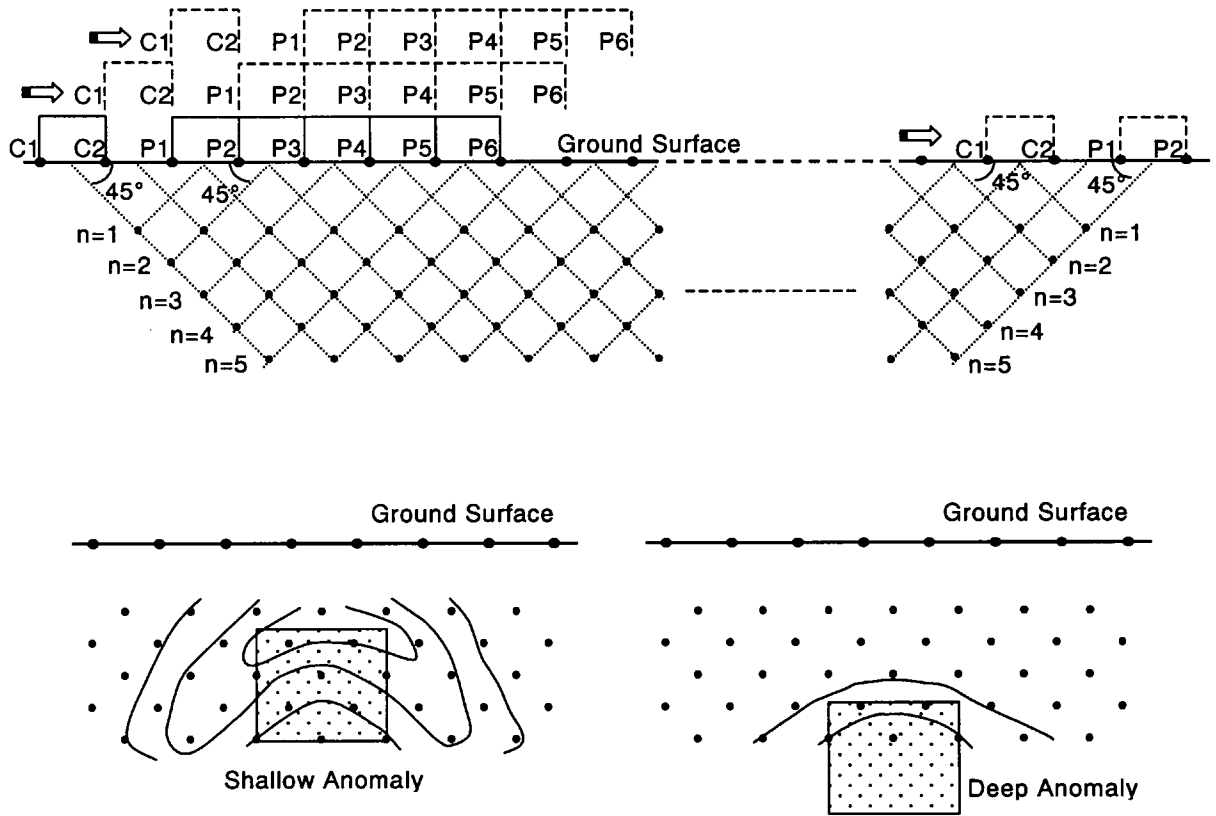
Figure 33 Plotting IP pseudo section with Dipole-Dipole Configuration
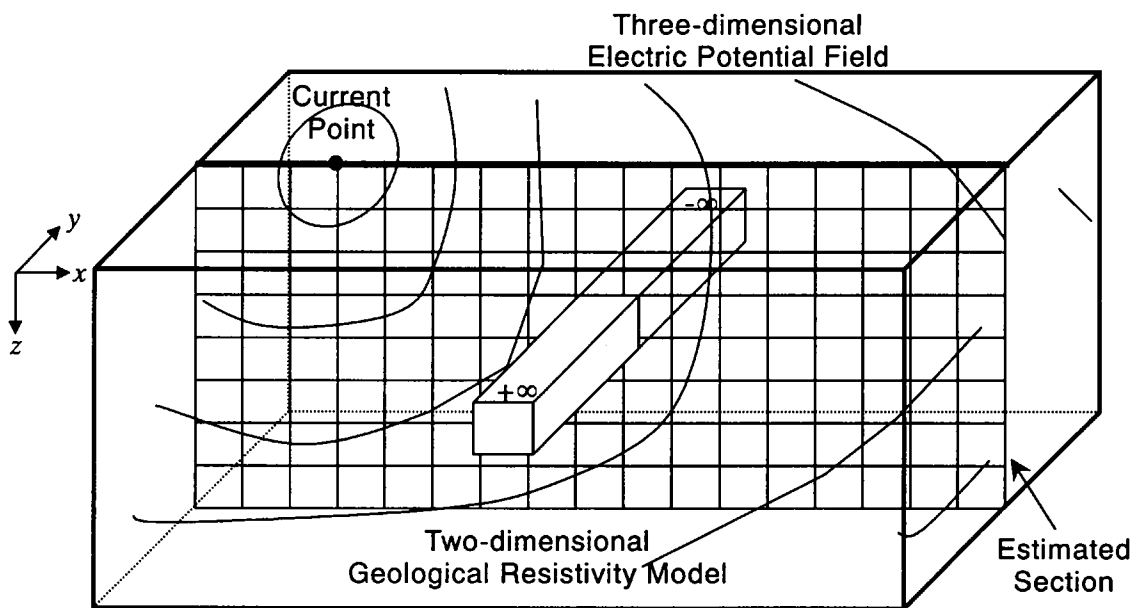and Typical Anomaly Pattern

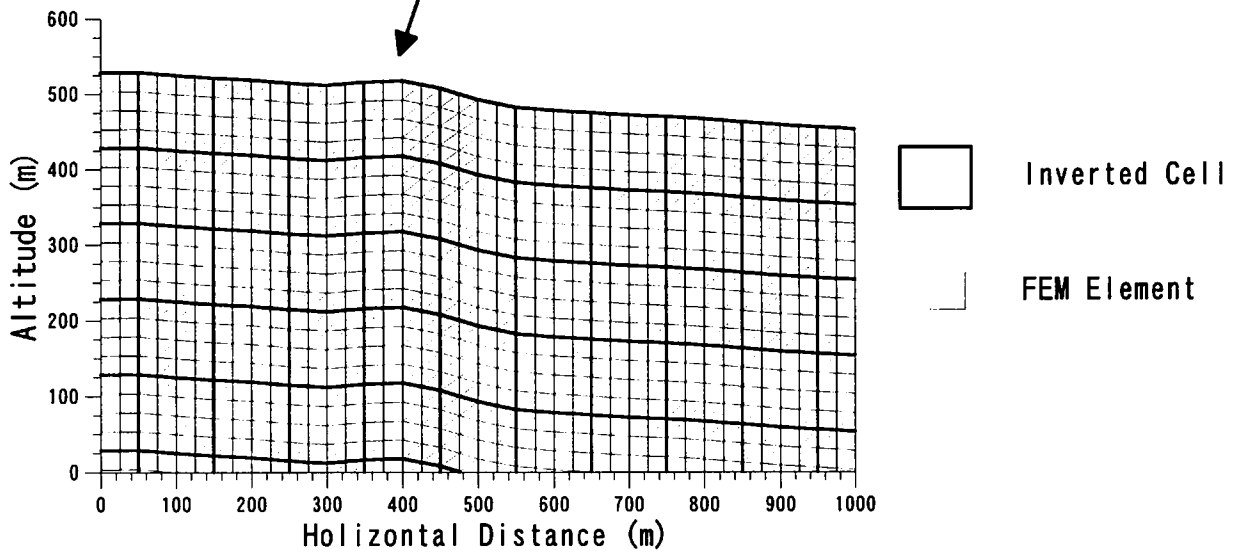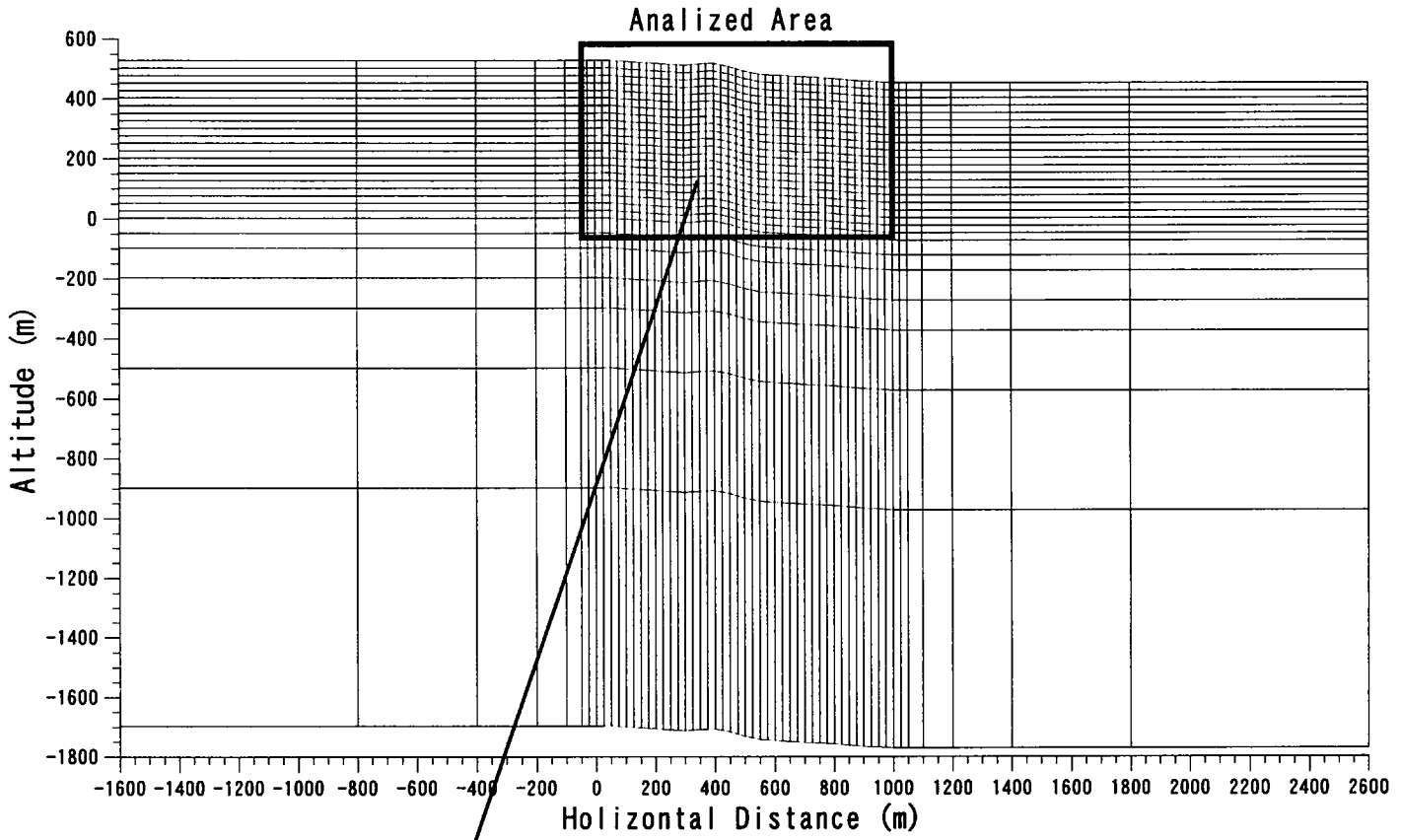**Figure 34** Schematic diagram of 2.5-D resistivity modeling
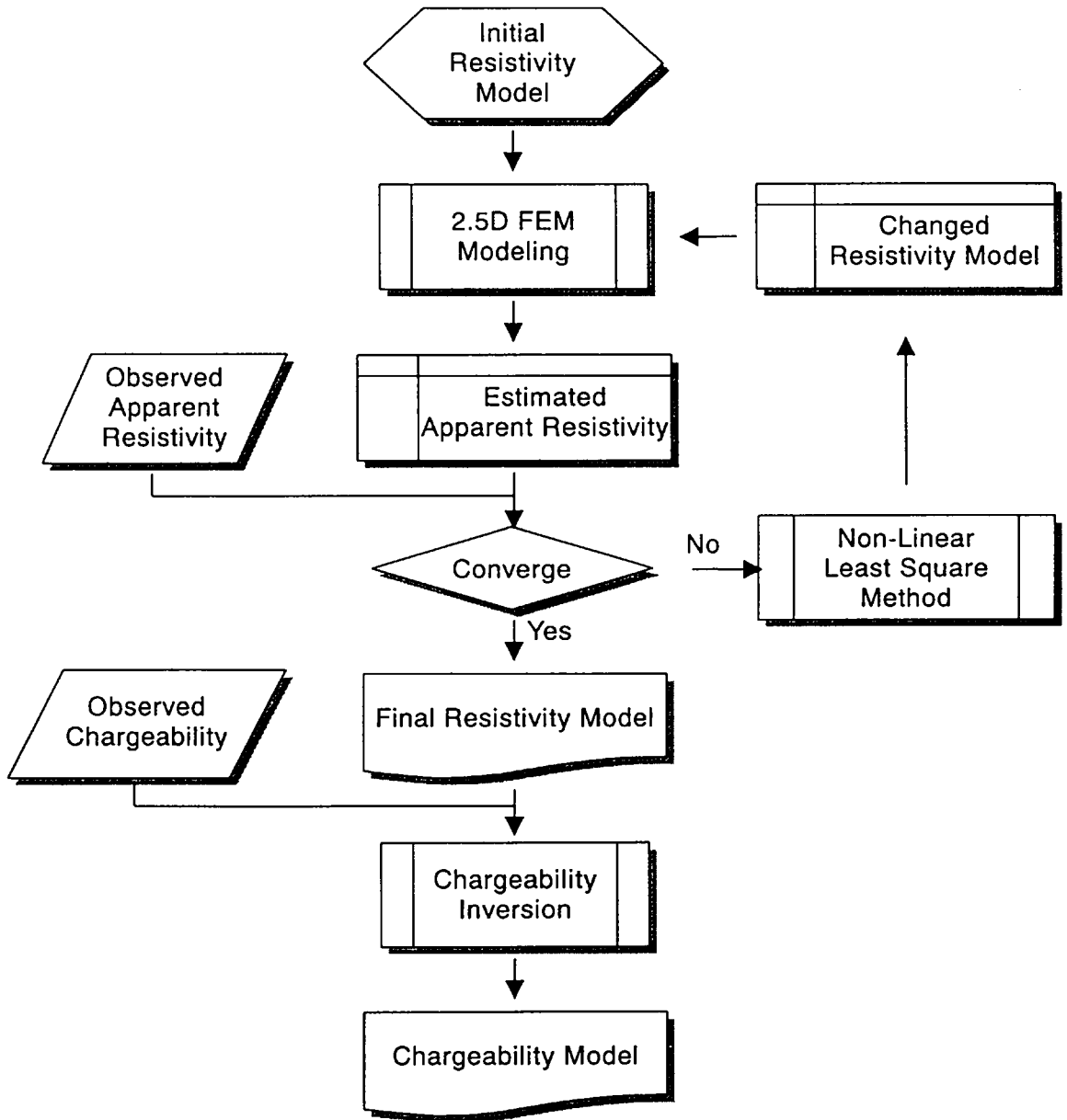
Figure 35　Mesh of 2.5D Finite Element Method

Figure 36 Flow chart of IP data inversion

(4) Laboratory Test

Density, apparent resistivity and chargeability are measured in laboratory for 21 samples collected from outcrops within and around the prospect and shaped into cylinders with a diameter of 3.5 cm and a length of 6.5 cm.

Weights of sample cylinders are measured in atmosphere and water under 1) natural condition, 2) enforced wet condition, after immersed in city water for more than 48 hours, and 3) enforced dry condition, after dried in a dry oven for more than 48 hours. Density is estimated using the equations, from (13) through (15). The result is collectively shown in Table 23.

$$\gamma_n = W1/(W2-W3) \tag{13}$$

$$\gamma_w = W2/(W2-W3) \tag{14}$$

$$\gamma_d = W4/(W2-W3) \tag{15}$$

Where,

γ_n: natural dry density,　γ_w: enforced wet density,　γ_d: enforced dry density

W1: weight in atmosphere under natural condition

W2: weight in atmosphere under enforced wet condition

W3: weight in water under enforced wet condition

W4: weight in atmosphere under enforced dry condition

Table 25 Results of Rock Density measurement of specimens in Bou Khil area

No.	Location	Geology	Rock	Weight (g)				Density (g/cm³)			Porosity (%)
				W1	W2	W3	W4	Natural	Dry	Wet	
1	B1-105	Trias	Lime Stone	160.05	97.95	158.20	157.95	2.55	2.54	2.58	3.4
2	B1-110	〃	Dolomite	172.20	109.85	168.65	167.70	2.70	2.69	2.76	7.2
3	B2-80	〃	Dolomite	168.60	105.95	166.05	165.90	2.65	2.65	2.69	4.3
4	B2-90	〃	Dolomite	157.75	94.10	149.35	148.45	2.35	2.33	2.48	14.6
5	B4-95	〃	Sand Stone	148.30	84.40	141.30	140.95	2.21	2.21	2.32	11.5
6	B6-60	〃	Mud Stone	155.45	98.35	153.30	152.25	2.68	2.67	2.72	5.6
7	B6-80	〃	Sandstone	127.55	64.40	121.40	100.40	1.92	1.59	2.02	43.0
8	B3-55	Transition	Lime Stone	153.85	94.75	151.10	150.45	2.56	2.55	2.60	5.8
9	B3-60	〃	Celestite	221.60	159.50	220.00	219.45	3.54	3.53	3.57	3.5
10	B3-60	〃	Celestite	257.80	190.25	257.05	256.70	3.81	3.80	3.82	1.6
11	B0-80	〃	Contact	137.05	80.15	127.90	126.65	2.25	2.23	2.41	18.3
12	B4-60	Cretacious	Lime Stone	178.40	115.05	178.30	178.20	2.81	2.81	2.82	0.3
13	B0-150	〃	Lime Stone	166.70	106.80	165.25	164.20	2.76	2.74	2.78	4.2
14	B3-70	〃	Lime Stone	163.65	100.00	160.10	159.75	2.52	2.51	2.57	6.1
15	B0-200	〃	Lime Stone	180.90	112.50	179.40	179.15	2.62	2.62	2.64	2.6
16	B1-75	〃	Lime Stone	147.40	90.60	146.05	145.70	2.57	2.57	2.60	3.0
17	B4-70	〃	Marl	165.85	102.75	164.75	164.10	2.61	2.60	2.63	2.8
18	B2-30	〃	Marl	161.90	97.70	158.10	156.80	2.46	2.44	2.52	7.9
19	B1-95	Tertiary	Sandstone	148.35	87.35	146.55	146.35	2.40	2.40	2.43	3.3
20	B1-75	〃	Sandstone	106.65	64.50	104.15	103.90	2.47	2.47	2.53	6.5
21	B0-100	〃	Sandstone	156.95	95.40	153.80	153.55	2.50	2.49	2.55	5.5

Apparent resistivity ρ and chargeability M are measured using the field equipment, XMT-32 and GDP-32, for sample cylinders held in GS type sample holders under enforced wet condition. The measurement device is illustrated in Figure 37. The equation (15) is used for estimation of apparent resistivity, while readings of the receiver are converted to chargeability using the equation (11), the same as for the field measurement.

$$\rho = (S/l)\ (V/I)$$

Where,   S: cross section area of sample, l: length of sample

V: received voltage (unit: V),   I: transmitted current (unit: A)
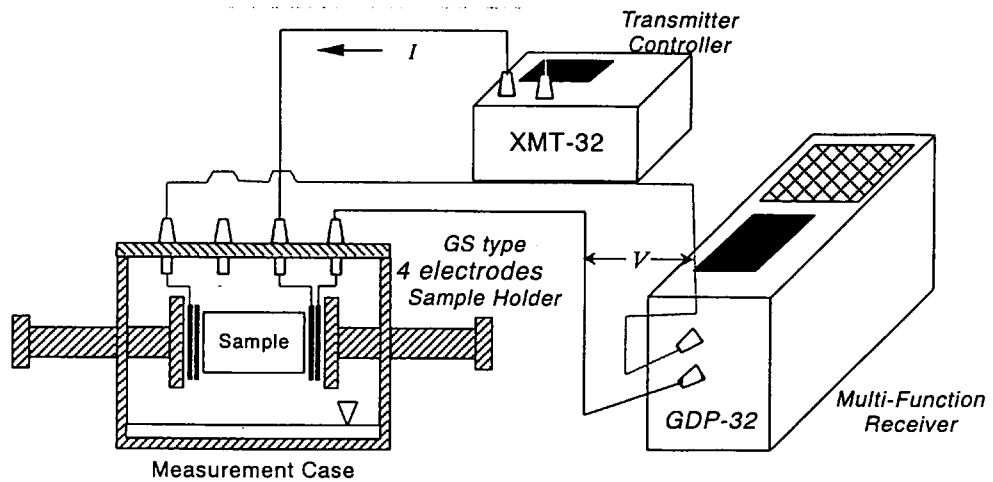
Figure 37 Schematic diagram of IP measurement for a rock sample

The result of apparent resistivity measurement is shown in Table 26. Two ore samples, collected from a waste dump of the old Bou Khil mine, are added for the apparent resistivity and chargeability measurement. Water , immersing the samples, indicated conductivity of 708 μS/cm, equivalent to 14.1 Ωm, at a temperature of 23° C at the time of measurement.

Table 26 Results of IP measurement of specimens in Bou Khil area

No.	Location	Geology	Rock	Diameter (mm)	Length (mm)	Current (μA)	Voltage (V)	Resistivity (Ωm)	Chargeability (mV/V)
1	B1-105	Trias	Lime Stone	35.35	64.00	5	0.6671	2046	7.32
2	B1-110	〃	Dolomite	35.10	65.60	2	0.9702	7155	7.54
3	B2-80	〃	Dolomite	35.35	64.55	5	1.0980	3339	1.11
4	B2-90	〃	Dolomite	35.50	66.00	5	0.4104	1231	1.43
5	B4-95	〃	Sand Stone	35.45	65.90	5	0.1737	520	11.73
6	B6-60	〃	Mud Stone	35.40	58.60	5	0.1465	492	0.14
8	B3-55	Transition	Lime Stone	35.35	61.10	5	0.4412	1417	3.05
9	B3-60	〃	Celestite	35.50	63.80	5	0.7405	2298	3.25
10	B3-60	〃	Celestite	35.40	70.00	5	1.9763	5558	1.11
11	B0-80	〃	Contact	34.50	60.00	5	0.4028	1255	1.14
12	B4-60	Cretacious	Lime Stone	35.40	65.70	5	3.4985	10482	8.86
13	B0-150	〃	Lime Stone	35.00	63.00	5	0.1370	419	5.08
14	B3-70	〃	Lime Stone	35.40	65.55	5	0.8620	2589	1.52
15	B0-200	〃	Lime Stone	35.90	69.10	5	1.2497	3661	3.02
16	B1-75	〃	Lime Stone	35.35	58.60	5	1.0920	3658	3.36
17	B4-70	〃	Marl	35.60	64.40	5	0.0980	303	2.11
18	B2-30	〃	Marl	35.60	65.70	5	0.0275	83	1.75
19	B1-95	Tertiary	Sandstone	35.55	63.30	5	0.7163	2247	3.88
20	B1-75	〃	Sandstone	35.20	44.80	5	0.0547	238	12.69
21	B0-100	〃	Sandstone	34.85	66.00	5	0.1680	486	5.98
22	B0-140	Ore	Galena	48.00	100.00	5	0.6807	2464	23.27
23	B0-140	〃	Gelena			5	0.2505		33.72

3.3.2 Gravity Survey

Characteristics of Bouguer anomaly(hereinafter called 'gravity') distribution are described below.

(1) Regional Gravity Distribution (Figures 38 and 39)

The NE-SW and crosscutting NW-SW gravity trends are predominated in the region including the Bou Khil prospect, reflecting the regional geological structure, according to the regional gravity distribution (Figure 38) as the result of CG-02 project. The Bou Khil prospect is located at the southeastern end of an extensive rectangular area of gravity high which is outlined by the 0 mgal contour and extends southeastward from the vicinity of the Lambert coordination of 420,000E and 350,000N. A zone of steep gravity gradient, bounding the southeastern end of the extensive gravity high, runs in the ENE-WSW direction near the western boundary of the prospect. The northeastern part of the prospect is situated on a saddle of a narrow gravity high stretching towards another gravity high in the southeastern part. The southern part lies in the marginal zone of an extensive gravity low which is outlined by the 0 mgal contour and trends in the NW-SE direction. From the view point of the regional gravity distribution as shown in Figure 39, the Bou Khil mine is located at the inflexion where the zone of steep gravity gradient, bounding the extensive gravity low,
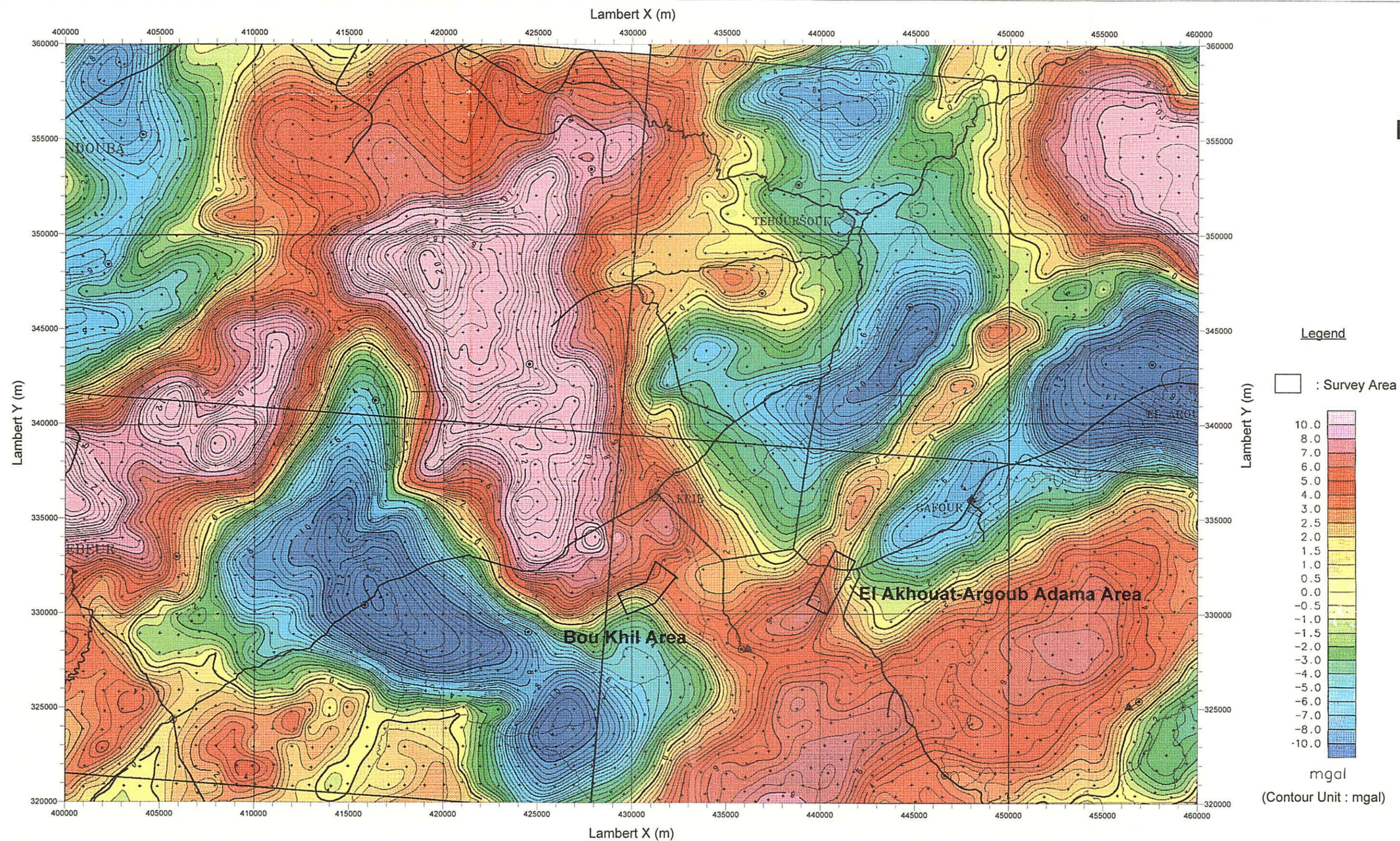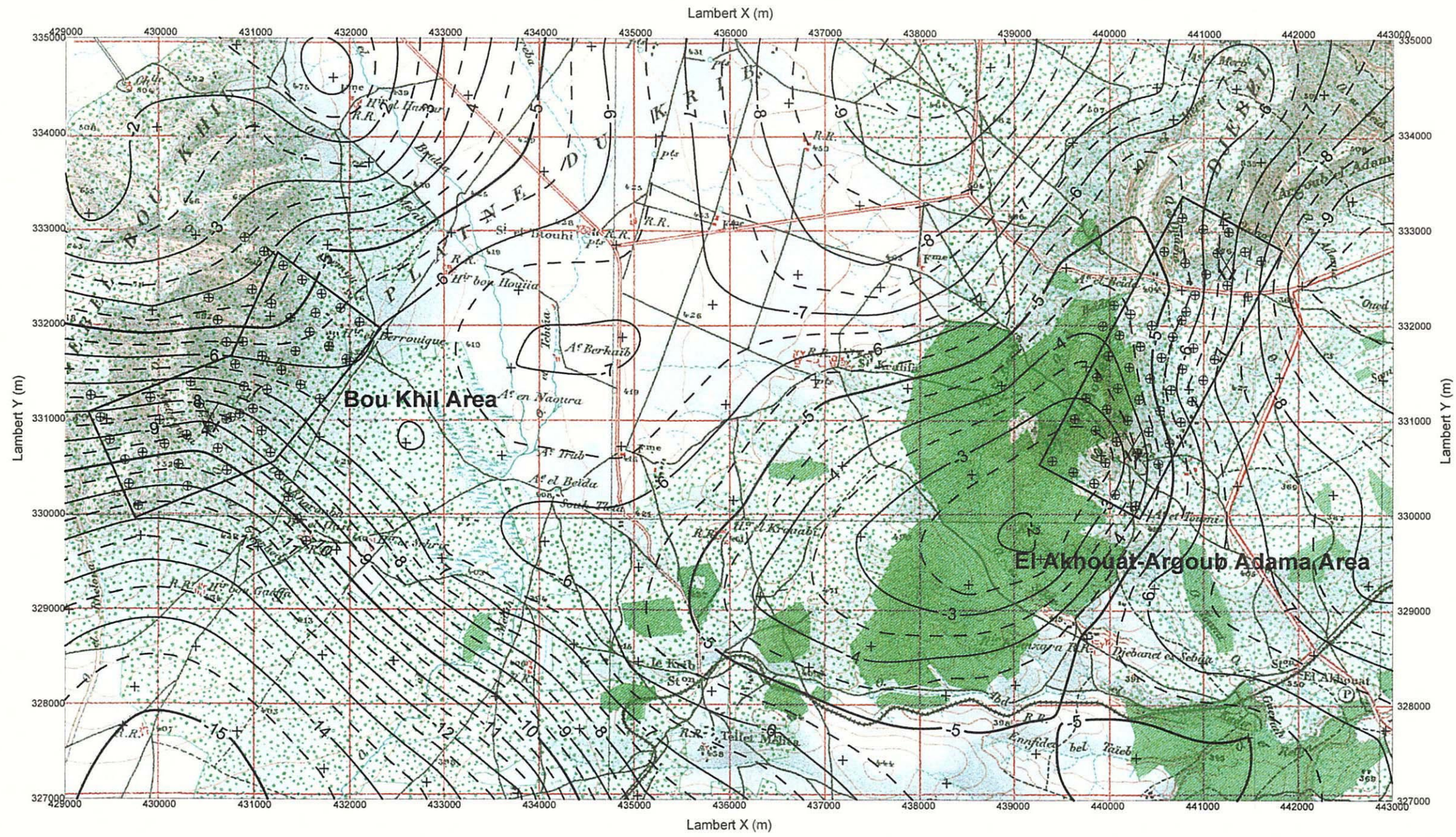
Figure 38

Reagional Bouguer Anomaly Map
(Density : 2.33 g/cm³)

Scale 1 : 200,000

March, 2000

Part of ONM, 1999

−76−

Lambert X (m)

Bou Khil Area

El Akhouat-Argoub Adama Area

Legend

⊕ : Gravity Station

+ : Existed Gravity Station

☐ : Survey Area

⋎ : Closed Mine

Figure 39

Regional Bouguer Anomaly Map
(Density : 2.33 g/cm^3)

Scale 1 : 50,000

March, 2000

changes its trend from the E-W direction to the NW-SE.

(2) Gravity Distribution of the Prospect (Figure 40)

The prospect can be principally divided into the northeastern and southern parts on the basis of the gravity distribution. The gravity in the northeastern part is relatively invariable, ranging between − 6 and − 5 mgal, and tends to become higher northwestwards. The southern part is situated in the transition zone from the northern part with relatively high gravity to the southern gravity low, and indicates swift decrease in gravity southwards from − 7 mgal to − 12 mgal. The contact between the Triassic and Cretaceous systems appears to correspond to a part of steep gravity gradient in the southern part, while no characteristic gravity feature is observed in association with the contact in the northeastern part. Therefore, it will be very difficult to identify the contact between the two systems based on the gravity distribution. As aforementioned, the Bou Khil mine is located at the inflexion of a zone of steep gravity gradient. In more detail, it appears also associated with a local gravity high jutting out southwards at its southern end. In association with this local gravity high, a celestite ore deposit is located to the north of the station B 0-100. The gravity high is bounded by the E-W line connecting the stations B 3-75 and B 0-175 for its southern limit.

(3) Residual Gravity Anomaly (Figure 41)

There are located four characteristic residual gravity anomalies in the prospect, two high anomalies exceeding 0.4 mgal in the central and western parts, and two low anomalies below − 0.2 mgal in the northern and southwestern parts. The triangular high residual anomaly centering the station B 4-75 corresponds to high density limestone of Cretaceous. Its southern margin trends in the ENE-WSW direction and is characterized by steep residual gravity gradient. The Bou Khil mine and the celestite deposit as above mentioned are located in this marginal zone of residual gravity anomaly. The high residual gravity anomaly in the vicinity of the station B 1-125 appears to indicate distribution of Triassic dolomite. These high residual gravity anomalies, together with the minor high in the vicinity of the station B 5-0, are aligned in the E-W direction. The low residual gravity anomaly in the northern part is open to the north and may reflect evaporite components of the Triassic system that are lower in density than other Triassic sedimentary rocks. The low residual gravity anomaly in the southwestern part can be correlated to Tertiary sedimentary rocks that are high in porosity and low in density. The 0 mgal contour appears to correspond to the contact between the Triassic and Cretaceous systems in the southern part. However, no specific feature of residual gravity is associated with the northern

contact, as is the case for the gravity distribution.

(4) First Vertical Derivative Gravity Anomaly (Figure 42)

The distribution of first derivative gravity is similar to that of residual gravity except for the northern part of the prospect. The first derivative gravity forms a high gravity anomaly in the northern part on the contrary to the residual gravity. The 0 mgal/km contour in the southern part can be correlated to the contact between the Triassic and Cretaceous systems. This contour runs in the WSW direction along the line B0 from the line B4 to B3 and then, to the west of the line B3, is shifted to the northwest by about 500 m. Therefore, a fault that dislocates the contact may be assumed between the lines B3 and B2. In the northern part, the Triassic-Cretaceous contact appears to follow the 0.003 mgal/km contour north northeastwards from the vicinity of the station 0-175. However, a relatively low zone of first derivative gravity with a width of about 200 m crosscuts the contact, running in the NW-SE direction along the northeast side of the line B5. This first derivative gravity low may suggest a certain structural break.

(5) Cross Section Analysis

① B-0 Cross Section (Figure 43)

This is a longitudinal section crosscutting the prospect along the base line from the southwest to the northeast. The gravity structure is principally two-layered, composed of a low density layer with density difference ranging from -0.10 to -0.11 g/cm^3 and the underlying gravity basement with density difference of 0.01 g/cm^3 that is correlated to Cretaceous limestone. The low density layer, with its bottom elevations ranging from 300 to 350 m, is about 200 m thick in average. However, the bottom falls to an elevation of approximately 50m between the stations B 0-10 and -60, with its thickness increasing to nearly 500m. The gravity basement is exposed on the surface between the stations B 0-70 and -110, thrusting over the low density layer. Celestite alteration is observed at the location corresponding to the gravity basement exposure. The gravity basement rises to an elevation of approximately 400 m, with thickness of the low density layer being reduced to about 50 m, between the stations B 0-150 and -210 where the old Bou Khil workings are located. The gravity basement abruptly falls to an elevation of about 200 m in the vicinity of the station B 0-220 in the northeast of the section. This depression of gravity basement may correspond to the first derivative gravity low extending northwesterly that is mentioned in the previous paragraph.

② B-1 Cross Section (Figure 44)

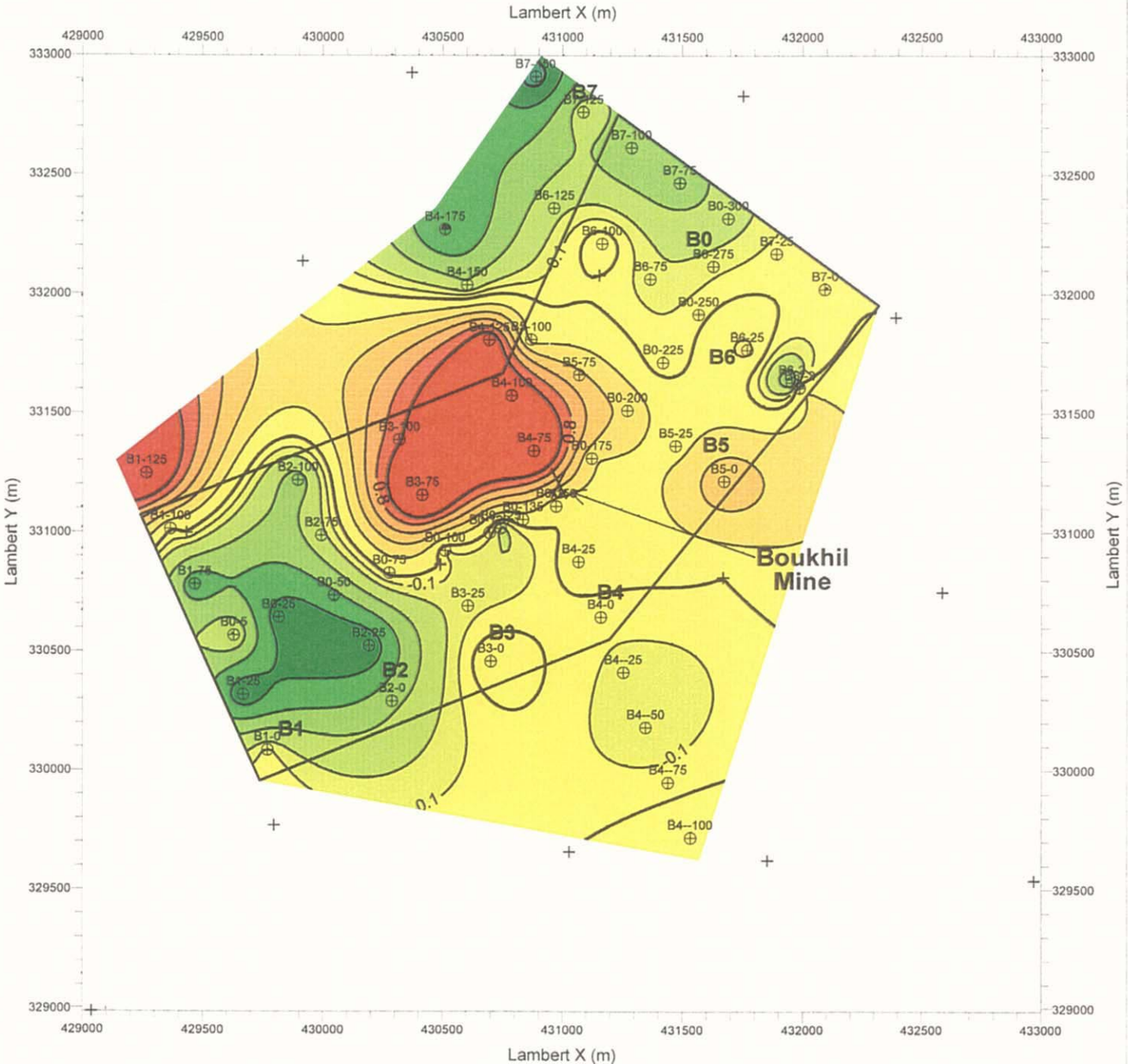This is the southwestern-most cross section, running in the NNW-SSE

Bouguer Anomaly Map in Bouhkil area
(Density : 2.33 g/cm³)
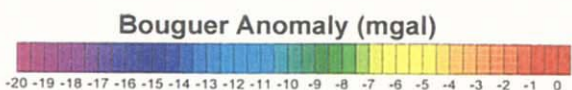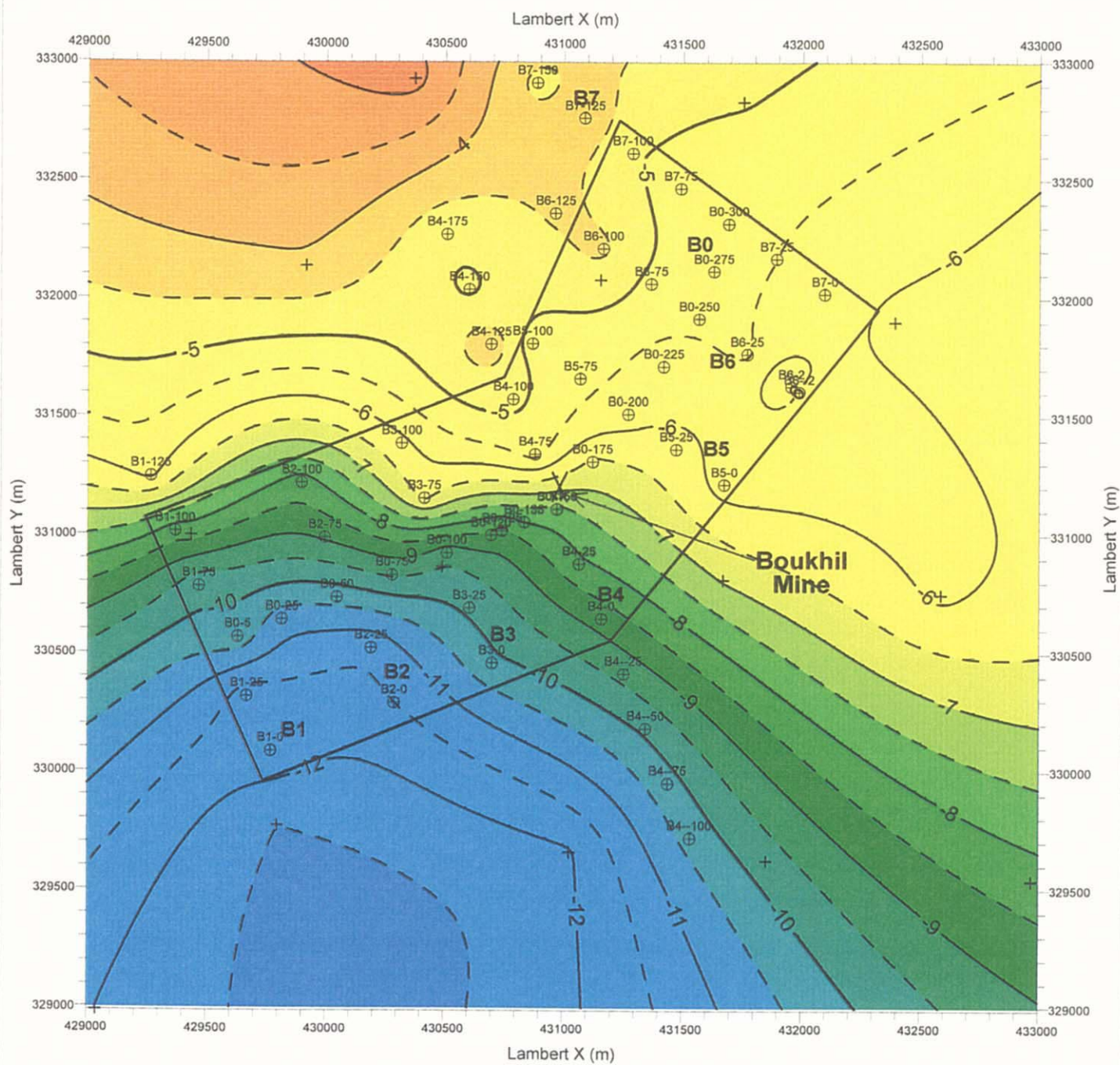
Legend

⊕ : Gravimetric Survey Station

— : IP survey Line

☐ : Survey Area

XX : Closed Mine

Figure 40

Bouguer Anomaly Map in Bouhkil area (Density : 2.33 g/cm³)

Scale 1 : 25,000

March, 2000

Figure 41

Residual Gravity Map in Bouhkil area (Density : 2.33 g/cm^3)

Scale 1 : 25,000

March, 2000

Legend

⊕ : Gravity Station

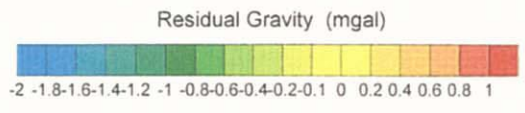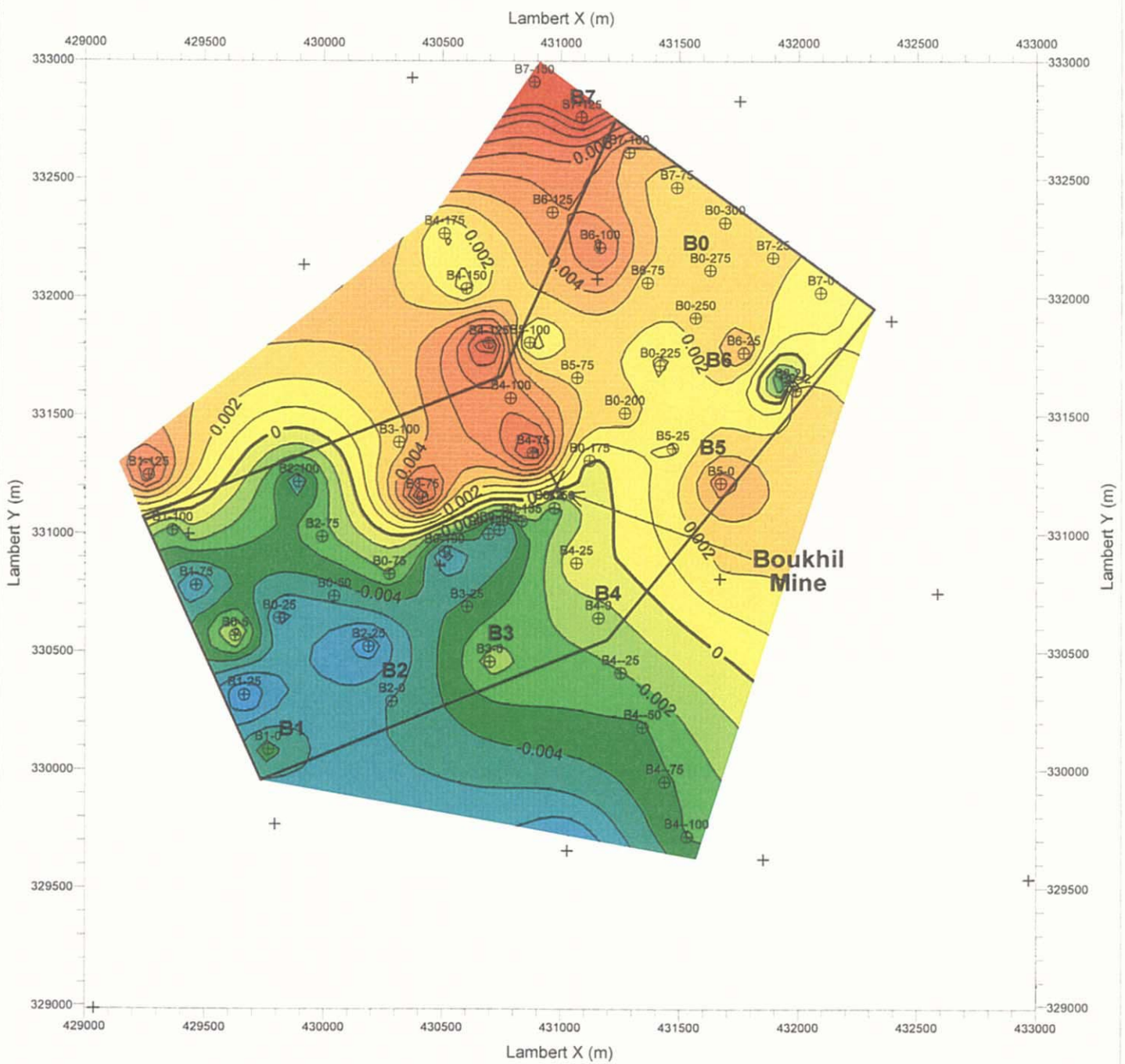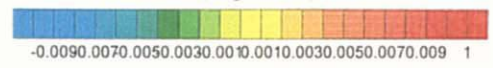+ : Existed Gravity Station

☐ : Survey Area

✗✗ : Closed Mine

Residual Gravity (mgal)

-2 -1.8 -1.6 -1.4 -1.2 -1 -0.8 -0.6 -0.4 -0.2 -0.1 0 0.2 0.4 0.6 0.8 1

Vertical Derivative Gravity Map in Bouhkil area

Legend

⊕ : Gravity Station

+ : Existed Gravity Station

☐ : Survey Area

X : Closed Mine

Figure 42

Vertical Derivative Gravity Map in Bouhkil area

Scale 1 : 25,000

March, 2000

direction. The gravity structure, the same as for the B 0 section except for its north northwestern end, is principally two-layered, composed of a low density layer with density difference ranging from − 0.10 to − 0.19 g/cm³ and the underlying gravity basement with density difference of 0.05 g/cm³. The low density layer, which may reflect Tertiary sandstone and conglomerate, is nearly 1,000 m thick from the station B 1-60 north northwestward, which is reduced to half as much, ranging from 400 to 600 m, to the south southeast of the station. The low density layer between the stations B 1-10 and -20 indicates particularly low in density difference at − 0.19 g/cm³, which may suggest a fault structure. A high density anomaly to the north northwest of the station B 1-110, which can be correlated to the Triassic system, indicates density difference at 0.11 g/cm³.

③　B-3 Cross Section (Figure 45)

This section crosscuts the southwestern part of the prospect in NNW-SSE direction. The gravity basement with density difference of 0.05 g/cm³ is rather deep-seated generally at elevations between − 300 and 0 m. However, it rises abruptly to an elevation of 200 m between the stations B 3-20 and −40, near the center of the cross section. In accordance with this basement rise, the overlying low density layer with density difference of − 0.10 g/cm³ reduces, from the south southeastern plain towards the center of the section, its thickness to about 250 m. This low density layer can be correlated to Tertiary sandstone and conglomerate. A low density anomaly with density difference of − 0.17 g/cm³ is located between the stations B 3-40 and -80 to the north northwest of the basement rise. A high density layer with density difference of 0.13 g/cm³ overlies this low density anomaly further to the north northwest and is correlated to Cretaceous limestone. A low density layer with density difference of − 0.12 g/cm³ is located near surface of the north northwestern end of the section, where the Triassic system is exposed. This is quite contrary to the case for the cross section B-1, in which the Triassic system is correlated to the high density anomaly. Celestite alteration is observed on the surface between the stations B 0-100 and B 3-70, about 100 m above the top of the low density anomaly.

④　B-4 Cross Section (Figure 46)

This section crosscuts the central part of the prospect through the old Bou Khil mine workings in the NNW-SSE direction. Distribution of density difference shows a similar pattern to that for the B-3 cross section. The depth of gravity basement with density difference of 0.06 g/cm³ ranges generally from 0 to 100m in elevation and rises to an elevation of about 300 m between the stations B 4-30 and B 0-150, to the south southeast of the old workings. A low density layer with density difference of − 0.28 g/cm³ develops over the gravity basement below a plain extending from the station

B 0-150 south southeastward. This low density layer can be correlated to the Tertiary system. A low density anomaly with density difference of -0.41 g/cm³ is located below the Bou Khil old workings and adjacent to the north northwest of the gravity basement rise. A high density block from the station B 0-150 to B 4-100 intervenes between the low density layer as above mentioned and another low density layer with density difference of -0.12 g/cm³ to the north northwest. The latter low density layer is correlated to the Triassic system. This high density block has similar density difference of 0.06 g/cm³ to that of the gravity basement and is correlated to Cretaceous limestone.

⑤　B-5 Cross Section (Figure 47)

This section crosscuts the central part of the prospect in the NW-SE direction, intersecting diagonally the B-4 cross section. The gravity basement with density difference of 0.02 g/cm³ occurs at elevations generally ranging from 0 to 200 m and rises to an elevation of 330 m from the station B 5-10 to the southeastern end. A low density layer with density difference of -0.05 g/cm³ overlies the gravity basement from the station B 5-60 southeastward and is correlated to the Tertiary system, over which a flat plain is developed on the surface. To the northwest of the station, a high density layer with density difference of 0.05 g/cm³ is developed, overlying the gravity basement and is correlated to Cretaceous limestone. No low density anomaly is observed in this cross section, differing from the B-3 and B-4 cross sections.

⑥　B-6 Cross Section (Figure 48)

This section crosscuts the northeastern part of the prospect in the NW-SE direction. The gravity basement with density difference of 0.02 g/cm³ stays at elevations ranging from -100 to 0 m to the southeast of the station B 6-60 and rises to an elevation of about 300 m to the northwest. A thin low density layer of some 100 m thick, indicating density difference of -0.06 g/cm³, is developed under a plain to the southeast of the station B 6-80 and is correlated to the Tertiary system. Under hilly terrain to the northwest, a low density layer with density difference of -0.01 g/cm³ overlies the gravity basement. A low density anomaly with density difference of -0.12 g/cm³ is located between the stations B 6-80 and -60 under the thin low density layer and adjacent to the gravity basement rise. A tip of low density layer with density difference of -0.14 g/cm³ blushes the northwestern corner near the surface.

(6) Interpretation of Gravity Plans

Characteristic residual gravity anomalies are superimposed over the first vertical derivative gravity contours at 0 and 0.003 mgal/km as shown in Figure 49.

The Bou Khil mine and the celestite alteration to the north of the station B 0-100 are situated along a belt of steep gravity gradient between a high residual
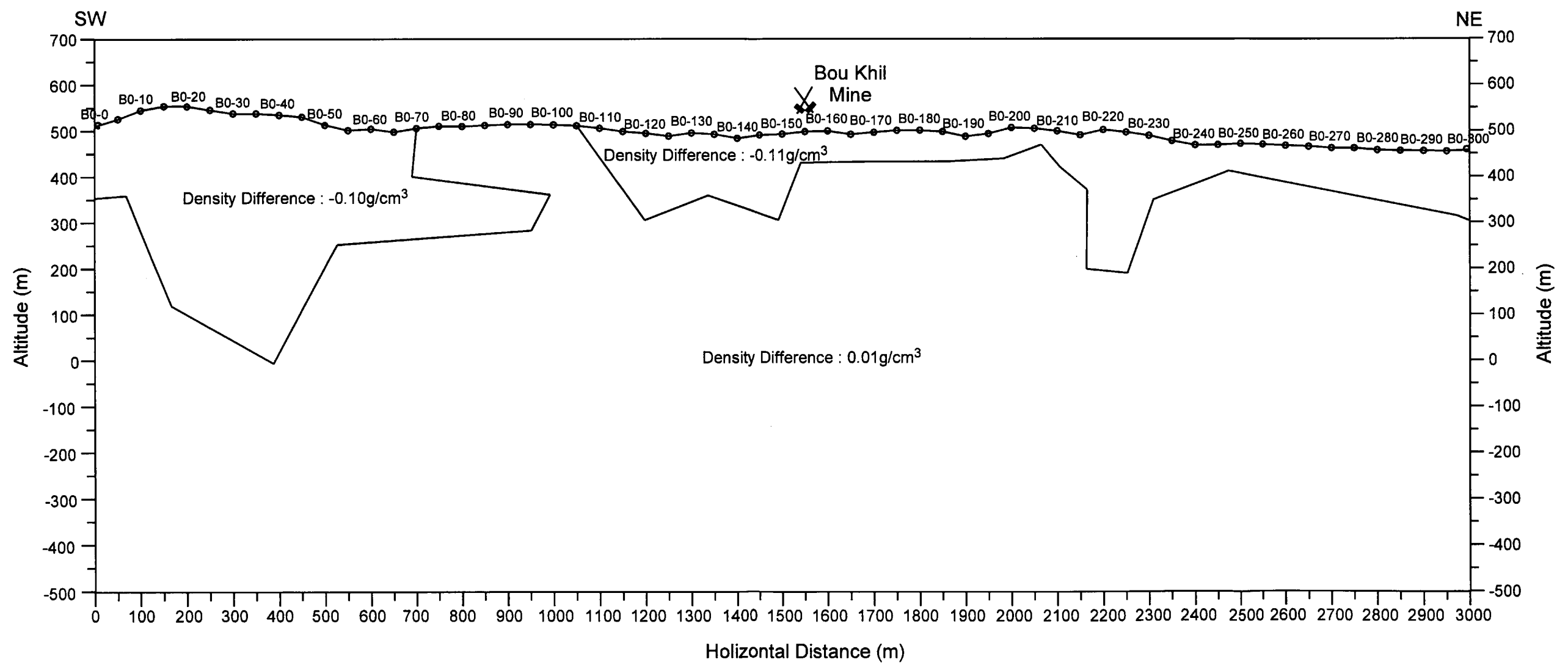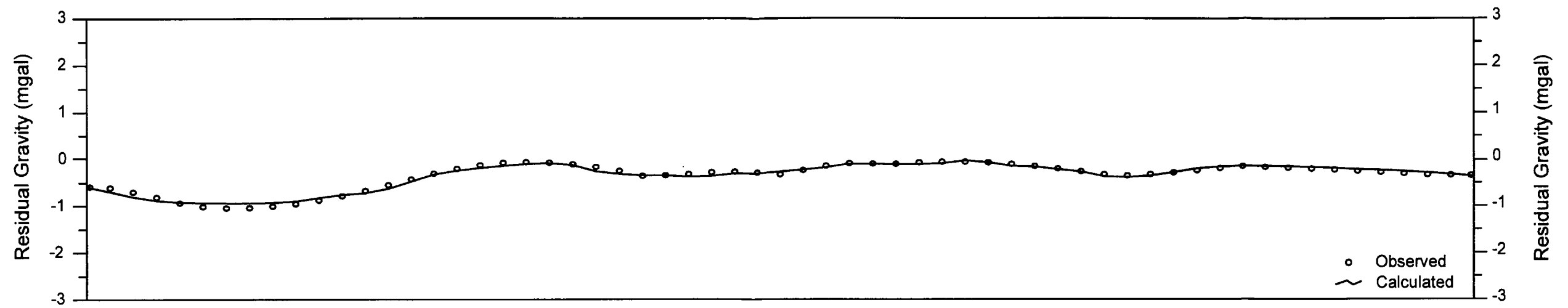
Figure 43

Result of 2-D Gravimetric analysis
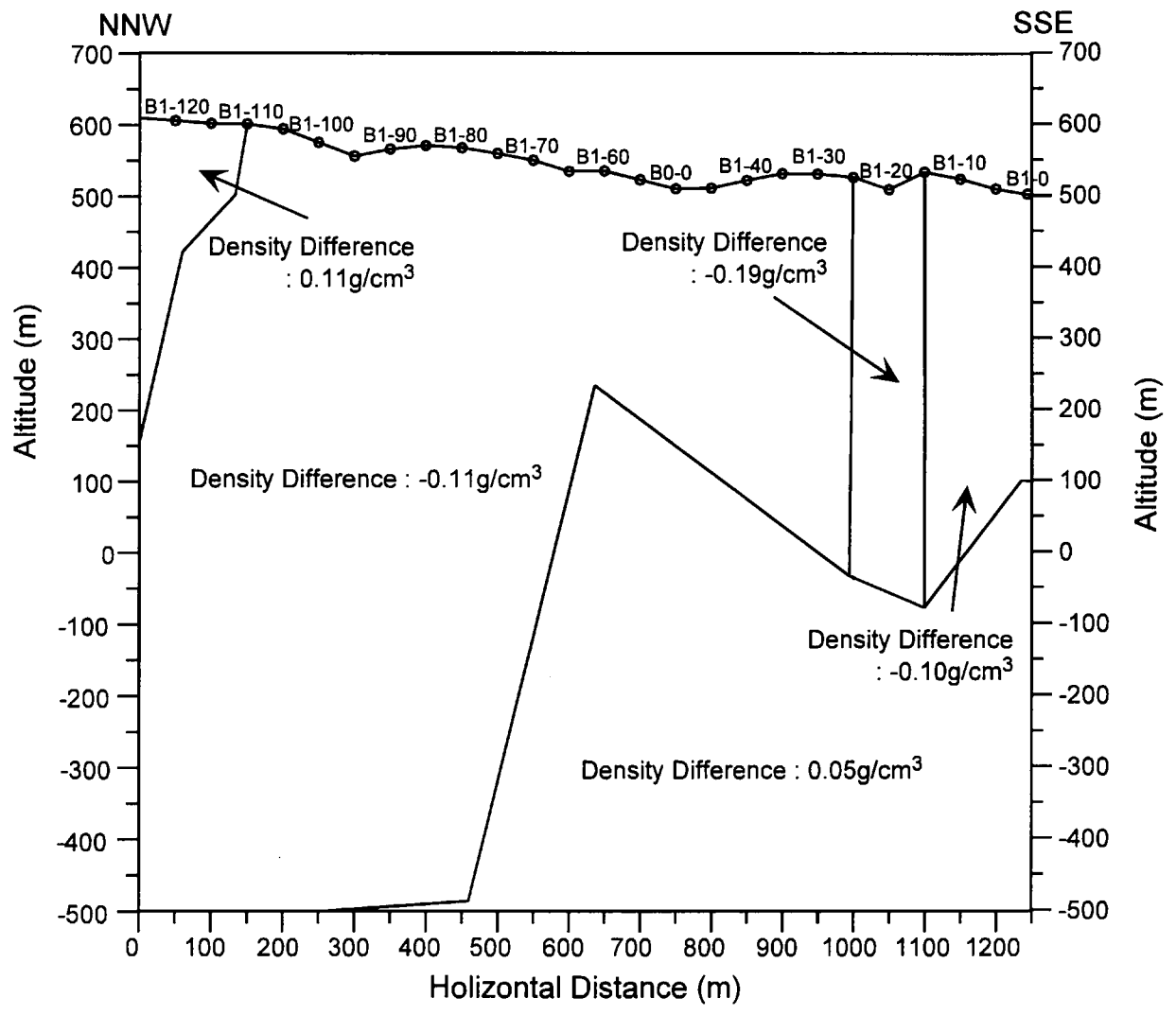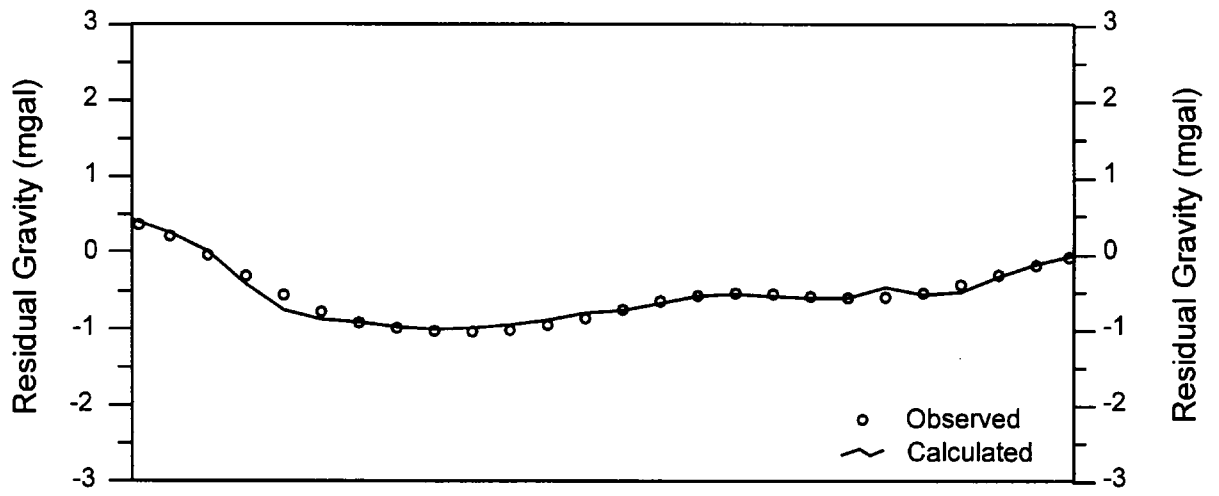(Line B0)

Scale : 10,000

March, 2000

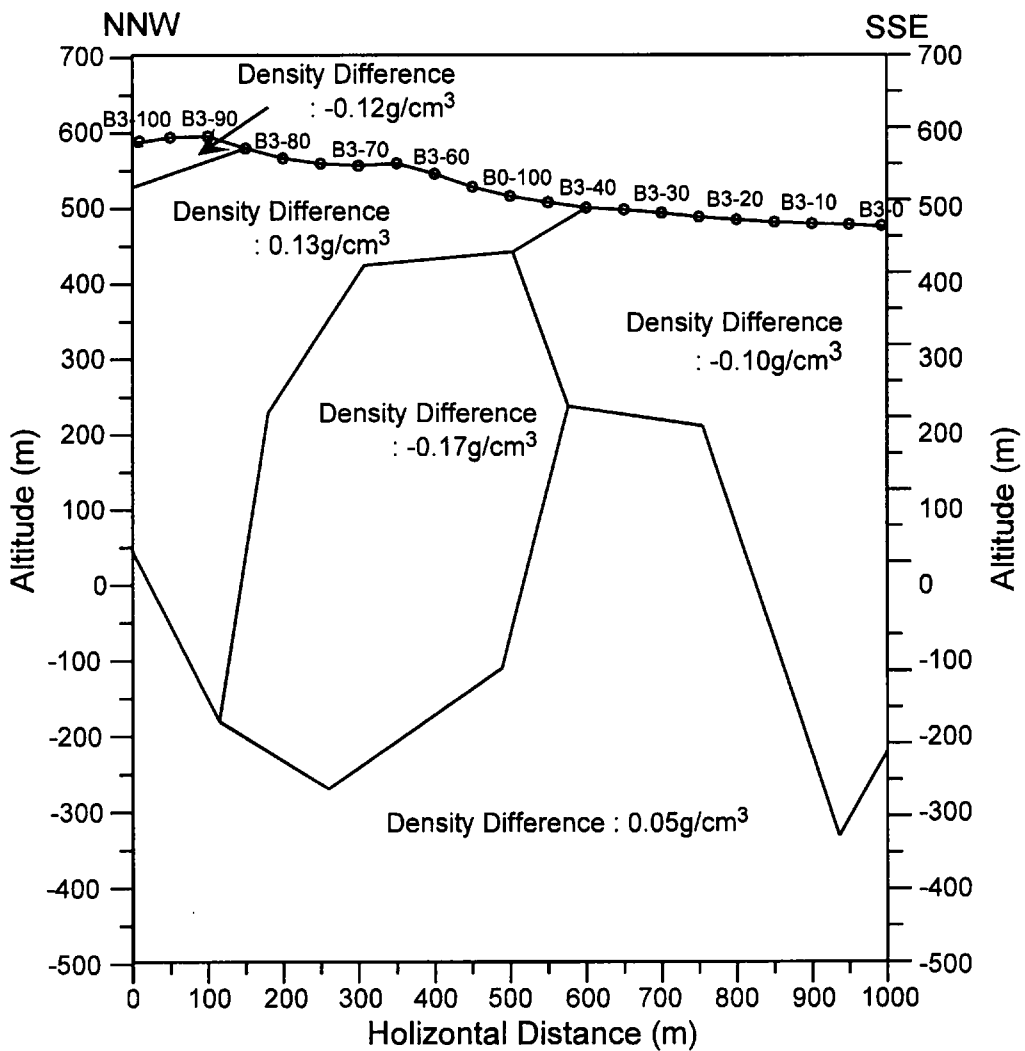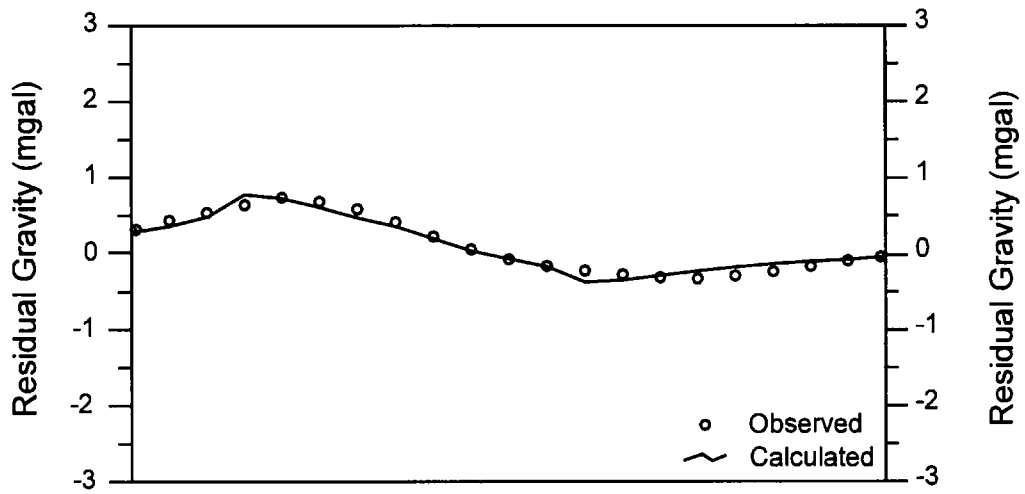|	Figure 44
	Result of 2-D Gravimetric analysis (Line B1)
	Scale : 10,000
	March, 2000

Figure 45

Result of 2-D Gravimetric analysis
(Line B3)

Scale : 10,000

March, 2000

Figure 46

Result of 2-D Gravimetric analysis
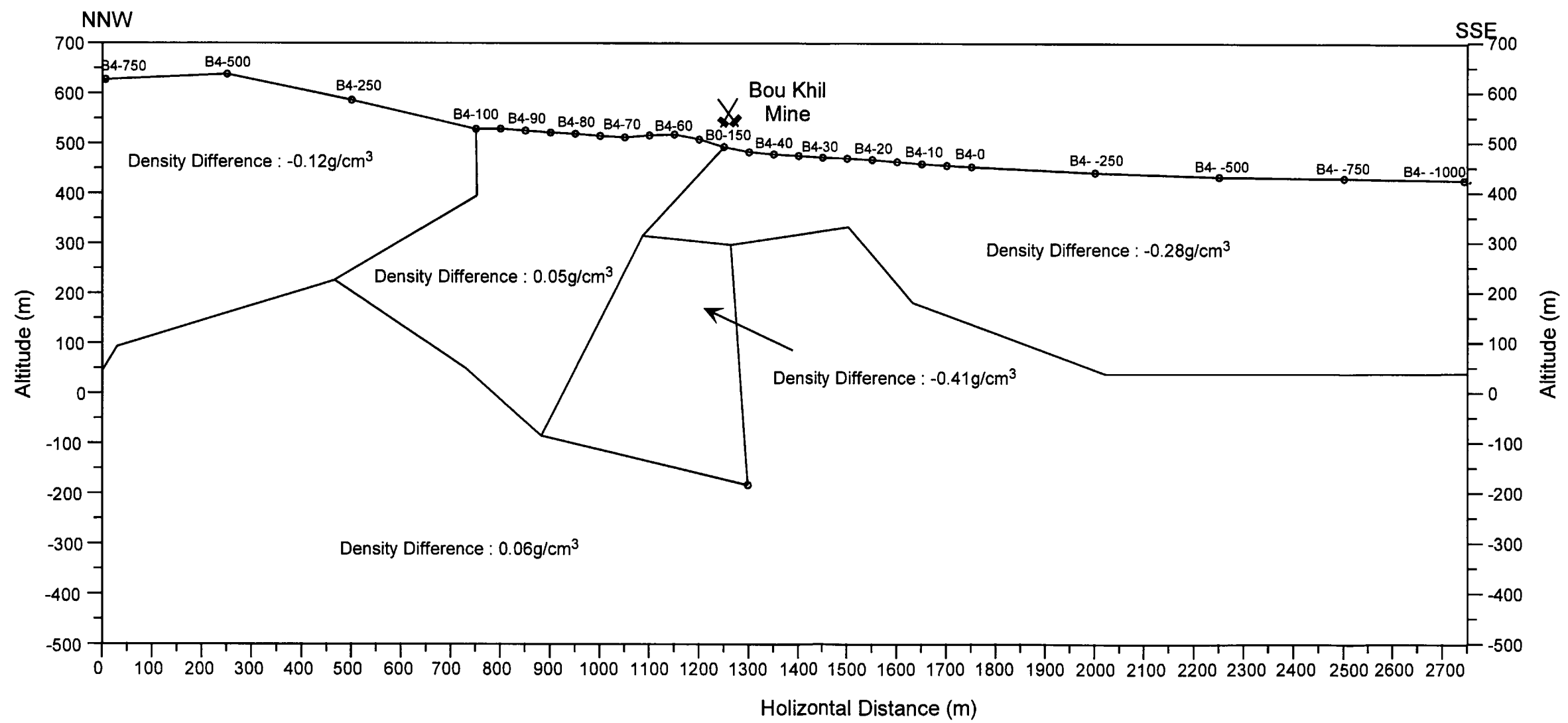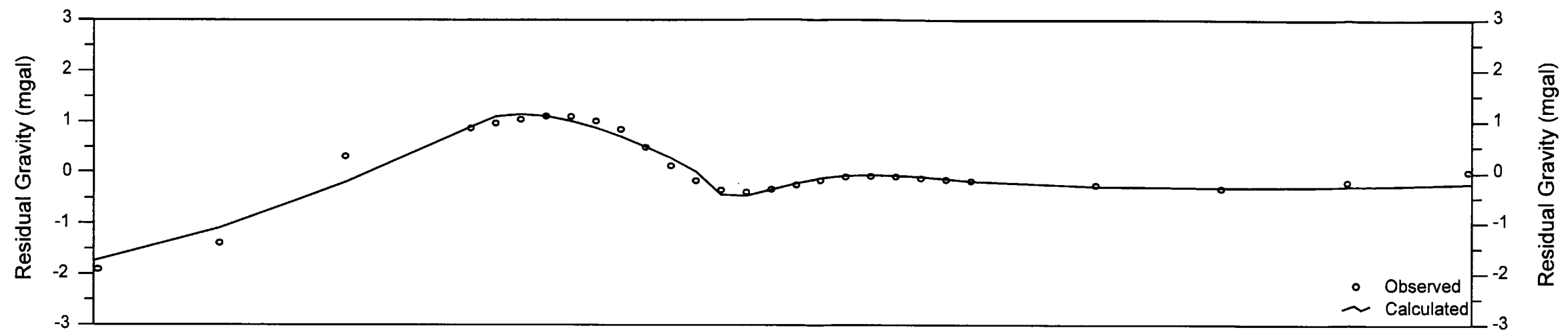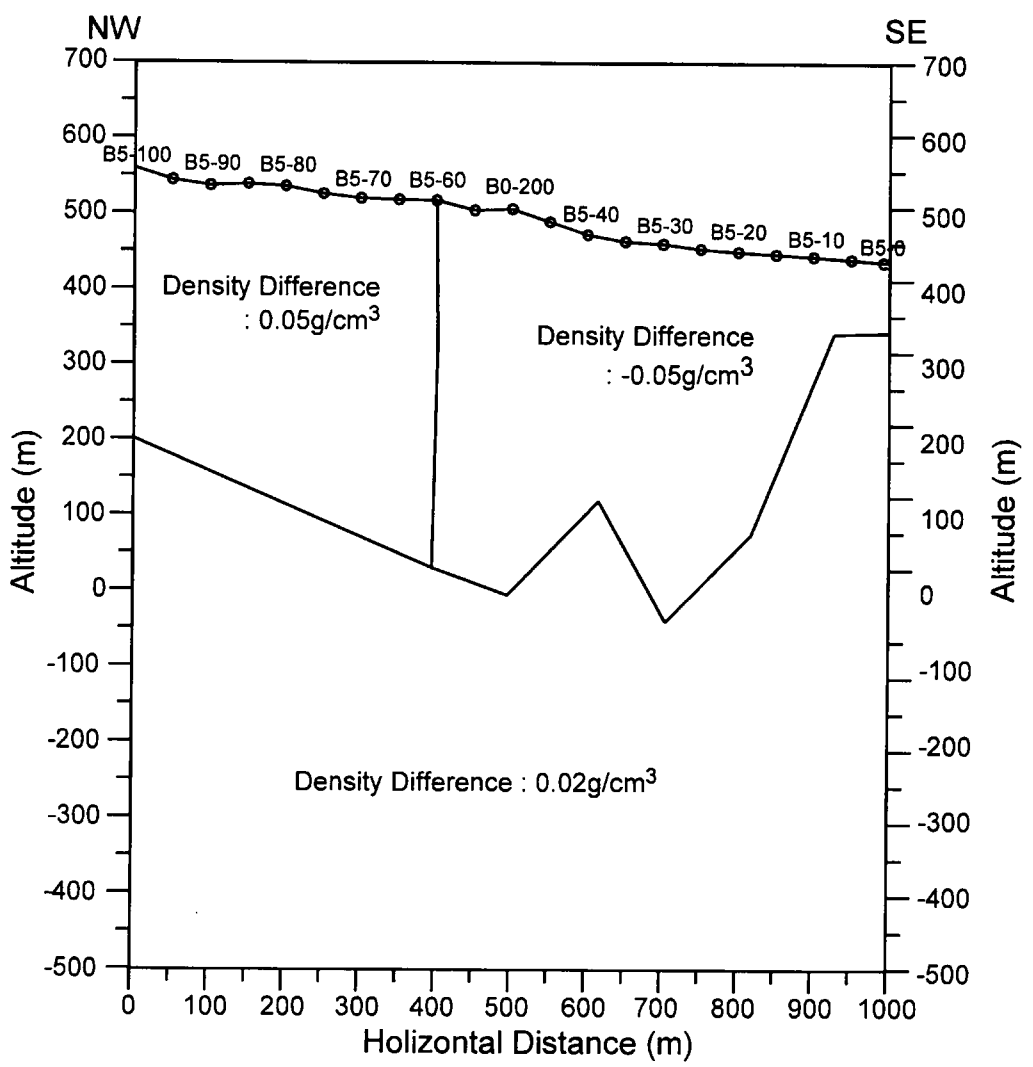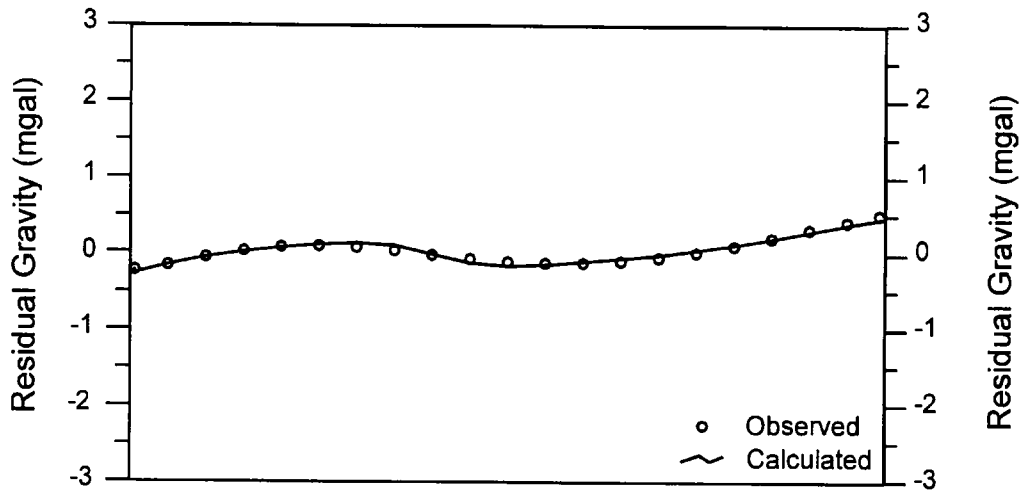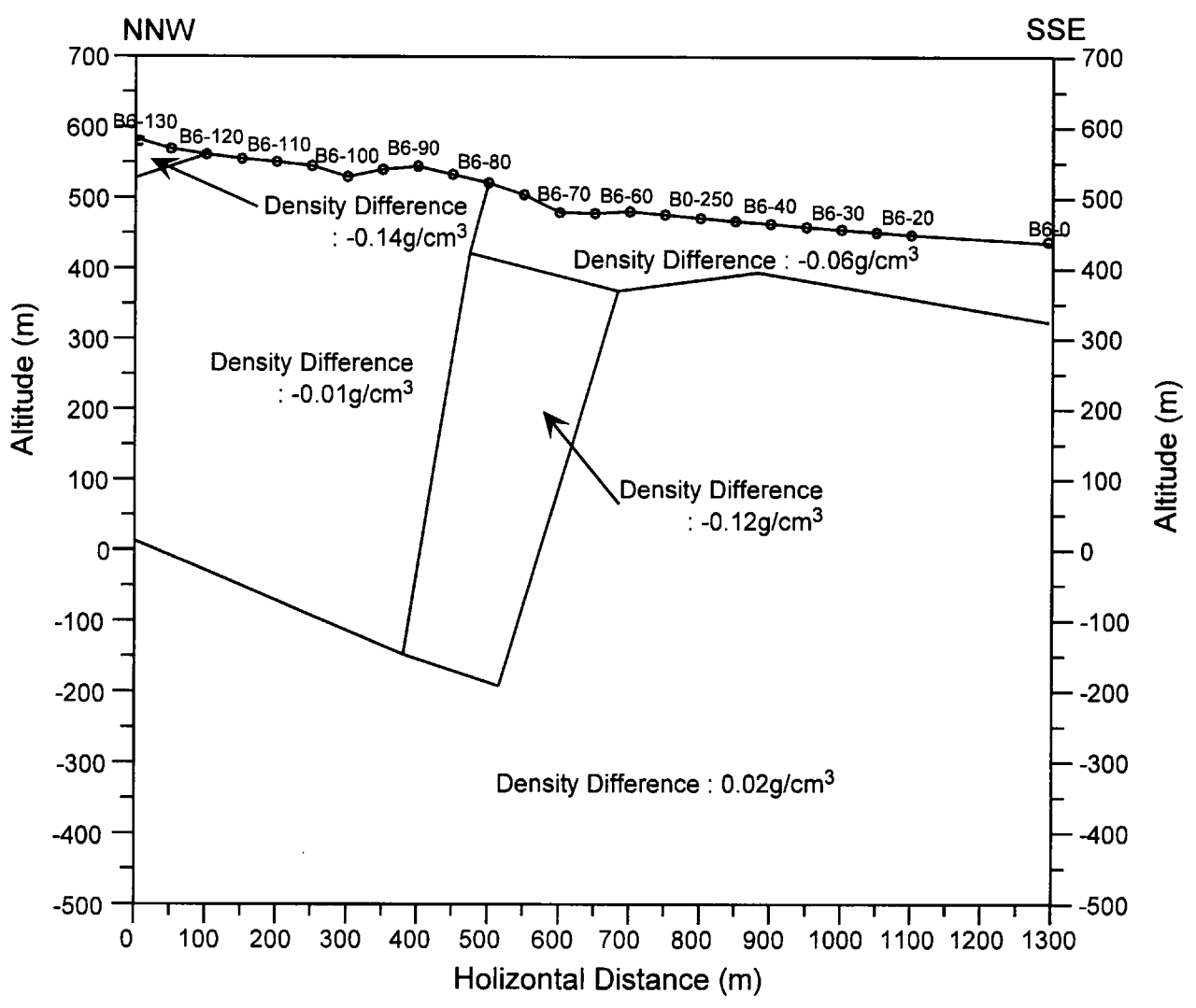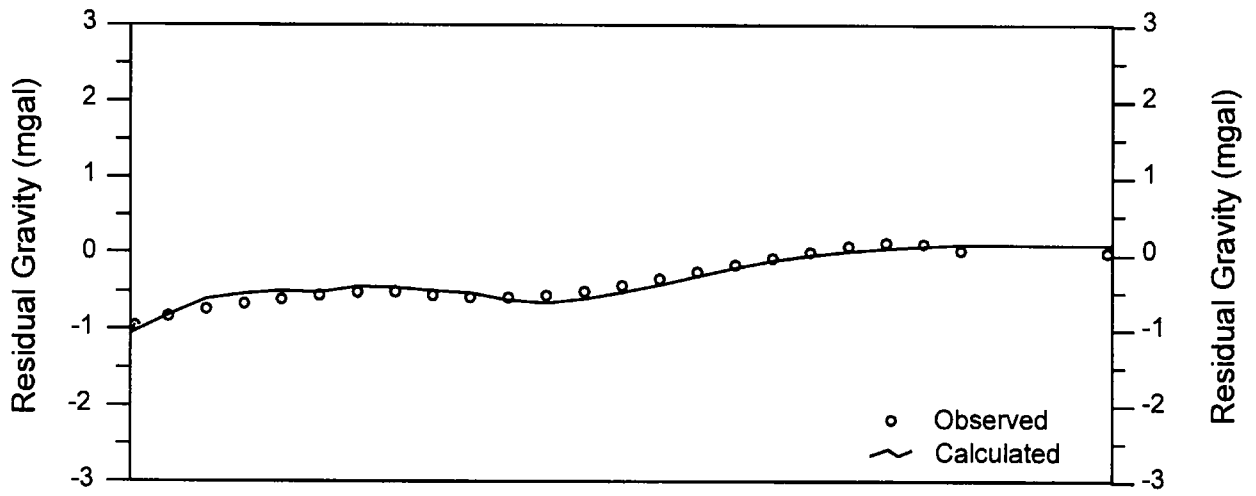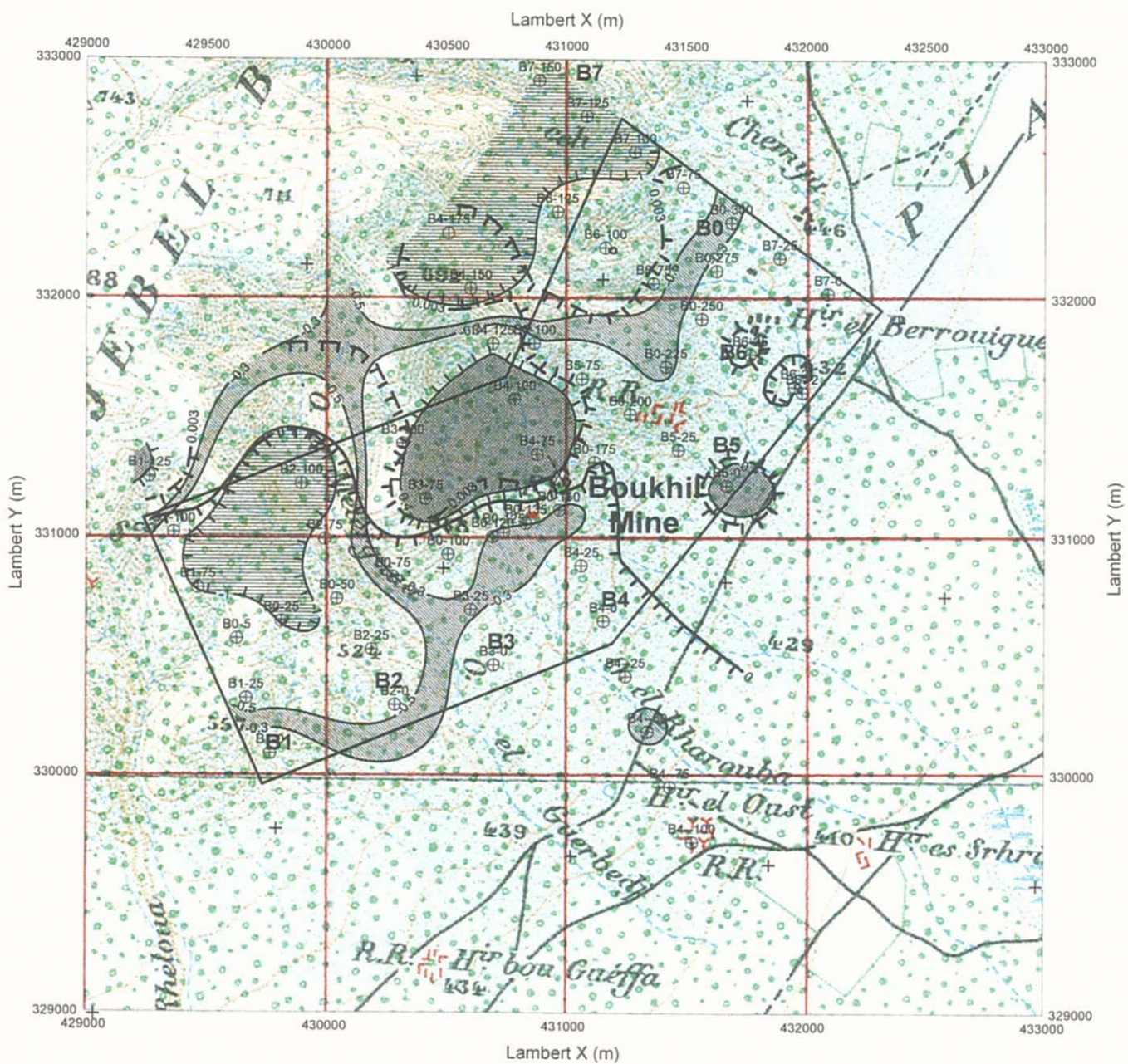(Line B4)

Scale : 10,000

March, 2000

Figure 47

Result of 2-D Gravimetric analysis
(Line B5)

Scale : 10,000

March, 2000

Residual Gravity (mgal)

- o Observed
- ~ Calculated

NNW   SSE

B6-130
B6-120 B6-110
               B6-100   B6-90
                                    B6-80
Density Difference   B6-70 B6-60 B0-250 B6-40 B6-30 B6-20
: -0.14g/cm³   B6-0
                                         Density Difference : -0.06g/cm³

Density Difference
: -0.01g/cm³

Density Difference
: -0.12g/cm³

Density Difference : 0.02g/cm³

Holizontal Distance (m)

| Figure 48 |
| Result of 2-D Gravimetric analysis (Line B6) |
| Scale : 10,000 |
| March, 2000 |

Figure 49

**Gravity Interpretation Map
in Bou Khil area**

Scale 1 : 25,000

March, 2000